OCCASION

This publication has been made available to the public on the occasion of the 50th anniversary of the United Nations Industrial Development Organisation.

DISCLAIMER

FAIR USE POLICY

CONTACT

Please contact publications@unido.org for further information concerning UNIDO publications.

For more information about UNIDO, please visit us at www.unido.org

UNITED NATIONS INDUSTRIAL DEVELOPMENT ORGANIZATION
Vienna International Centre, P.O. Box 300, 1400 Vienna, Austria
Tel: (+43-1) 26026-0 · www.unido.org · unido@unido.org

17363

DEVELOPMENT of RAPIDLY SOLIDIFIED AMORPHOUS and CRYSTALLINE ALLOYS

by

Géza Konczos

Central Research Institute for Physics, Hungarian Academy of Sciences, 1525 Budapest P.O.Box 49, Hungary

The report was prepared for UNIDO under agreement no. CLT 88/144

2a/

Budapest, October 1988

DEVELOPMENT of RAPIDLY SOLIDIFIED AMORPHOUS and CRYSTALLINE ALLOYS

by

Géza Konczos

Central Research Institute for Physics, Hungarian Academy of Sciences, 1525 Budapest P.O.Box 49, Hungary

The report was prepared for UNIDO under agreement no. CLT 88/144

Budapest, October 1988

Content

	page
1. INTRODUCTION	1
2. RAPID SOLIDIFICATION PROCESSES	2
2.1 Preparation of ribbons	2
2.1.1 Single roller processes	3
2.1.2 Twin roller processes	6
2.2 Preparation of wires	6
2.3 Preparation of powders	7
2.3.1 Atomisation	7
2.3.2 Diminution of RS ribbons	9
2.4 Surface melting processes	10
3. AMORPHOUS ALLOYS: PROPERTIES and APPLICATIONS	11
3.1 Fundamentals	11
3.1.1 Atomic structure	11
3.1.2 Thermal properties	13
3.1.3 Structural relaxation	16
3.1.4 Electrical properties	16
3.1.5 Magnetic properties	16
3.1.6 Mechanical properties	17
3.1.7 Chemical properties	17
3.2 Application of metallic glasses	20
3.2.1 Soft magnetic materials	20
3.2.2 Brazing filler materials	23
4. RAPIDLY SOLIDIFIED CRYSTALLINE ALLOYS	24
4.1 Constitutional and microcrystalline features of rapidly solidified alloys	25
4.2 Application of RS crystalline alloys	30
4.2.1 High performance structural materials	30
4.2.2 Tool and bearing materials	31
4.2.3 Iron-based magnetic alloys	32
4.2.3 Others	35
5. CONCLUSIONS	36
REFERENCES	37
Appendix I. Sources of information on rapid solidification	43
Appendix II. List of RS products and manufacturers	46

1. INTRODUCTION

The solidification of metallic melts is one of the most important processes determining the properties of solid metals and alloys. It has been studied intensively for many years /1/. In the early fifties the interest was focused on the distribution of impurities and alloying elements during crystallization, or the morphology of solid-liquid interface, etc. As a practical result of these studies, high purity metal and semiconductor crystals have been grown by zone melting and other techniques.

A new period began in 1960 when P. Duwez and his coworkers prepared Au-Si alloys, having amorphous atomic arrangements, by extremly rapid (10^5 K/s) solidification of small droplets of the melt on a cooled substrate /2/. For one or two decades the glass forming alloys (metallic glasses or glassy metals) were in the center of interest: their formation, structure, special properties and possible applications have been studied in many laboratories all over the world.

Since the end of the seventies the rapid solidification technologies have been applied for the production of commercial alloys, e.g. iron-, aluminium-, and titanium based alloys, too. These alloys are referred frequently as "microcrystalline", because of their fine grain size.

The benefits of rapid solidification can be divided into two categories. First of all, the rapid solidification extends the formation of new, metastable phases, increases the solubility of a few alloying elements, can refine the grained microstructure or, in special cases glassy structure. This can lead to better physical and chemical properties or unusual combinations of these. Secondly: the rapid solidification of the metallic melt is a one-step process by which alloys of small cross section (ribbon, wire, powder) can be produced directly from the melt, without any, expensive working and processing. In this sense, the rapid solidification technologies can be regarded as an extreme case of continuous casting.

New metastable states can be formed not only from melts but by such [illegible] implantation, ion bombardement, mechanical alloying [illegible] diffusion. These methods are still in the research stage and they are out of scope of this survey.

Since 1970 the rapid solidification technologies have been intensively studied in many countries, especially in the USA, Japan and Western-Europe. International journals, specialized conferences deal with the progress in this exciting field of research and development. The commercialization of metallic glasses began more than 10 years ago. In 1980, Battelle's Columbus Laboratories established the Rapidly Solidified Materials (RaSoMat) Resource Center where more than 8.000 published items have been collected.

The present survey consists of four chapters. After a short introduction (Chapter 1.) the most important types of rapid solidification processes are reviewed (Chapter 2.). The application of metallic glasses and microcrystalline alloys are discussed in Chapter 3. and 4., respectively. In the Chapter 5. some conclusion is drawn. Information on technical literature (monographs, proceedings) and on rapidly solidified /RS/ products are collected in Appendices I and II.

2. RAPID SOLIDIFICATION PROCESSES

[illegible] of metallic melts requires high cooling rates, [illegible] 10^2 K/s. Due to heat-conduction considerations there is a limiting thickness for any given cooling rate, typically 10 mm for 10^2 K/s, [illegible] mm for 10^6 K/s and 1 μm for 10^{10} K/s /3-4/. Usually ribbons, wires, [illegible] powders are produced, either with amorphous structure [illegible] with very fine crystalline grain size. By consolidation of powders larger parts can be obtained.

In this chapter the most important types of RS processes are shortly reviewed. Special emphasis is laid upon methods which have practical importance. The classification is based on the geometry of products.

2.1. Preparation of Ribbons

Recently, the majority of RS metals are produced in ribbon form. Several methods have been suggested for strip casting, but all the commonly used ones have a few similar features: the molten metal is brought into contact with a cooling, thermally good conducting substrate which serves as an effective heat sink /5/. Frequently, the melt is poured onto the substrate through a nozzle. Among the [illegible] the single and twin roller techniques are the most popular.

[illegible] jet processes the substrate is a rotating wheel. The [illegible] of this method is the so called chill-block melt spinning (CBMS) or the jet melt-spinning (FJMS) method where a free melt jet is [illegible] into the inside of a rotating drum /6/ or on the outer surface of a rotating copper disk /7/. The scheme of this latter method is given in Fig.1. Usually the metal is melted in a quarz nozzle by induction heating under an inert gas atmosphere. A free melt jet is formed which is impinged on the wheel. The jet then flattens, it forms a puddle on the substrate, and after a short "residence distance" the ribbon is separated from the wheel. Due to the instability of the puddle, relative narrow ribbons typically of 1-3 mm width, can be produced. The thickness is mainly controlled by the rotation speed (usually 10-30 ms^{-1}) and the overpressure of [illegible] (ranging from 50 up to several hundreds of millibars). The wheel is a copper disk, diameters of 100-200 mm are typical. The charge is not more than 100 grams. The role of processing parameters has been intensively studied by several authors /8-10/.

The CBMS method is typically a laboratory size method, however, several manufacturing processes are based on it and it played a very important role in the study of rapid solidification phenomena. Recently, hundreds of such small scale melt spinning equipments are working in research laboratories and universities.

Wider ribbons can be produced by the planar flow casting (PFC) process /11/. In this case the molten metal is poured onto the surface of a chilled block through a special nozzle which is placed near the surface of the block (Fig.1 b). The melt pool is stabilized by this arrangement. The nozzle - wheel gap is small, typically some tenths of a millimeter. The nozzle slit is usually rectangular, a value of 10-25 x 0,5-0,6 mm^2 is typical. A laboratory size PFC equipment is shown in Fig.2. The wheel is water-cooled, its diameter is about 250 mm, the width is about 30 mm. The metal is melted in a quarz nozzle (Φ 35 x 150 mm). About 500 g of metal can be melted in one run. The melt temperature is measured by an optical pyrometer.

On a laboratory scale (1-2 kg batch, 20 to 60 mm wide ribbons), the realization of this technique is relatively simple. In a pilot-plant or [illegible], however, the procedure becomes more complicated: the crucible and the nozzle are spatially separated, there must be an appropriate cooling of the rollers, the ribbon thickness has to be controlled, the simultaneous winding of the ribbon has to be ensured, etc. As a consequence of the erosion of the nozzle by the liquid metal, boron nitride or oxide ceramic nozzles are used instead of quarz. Recently several companies have solved these technical problems producing 150 to 500 kg of melts or even more.

[illegible] of the manufacturing equipment developed by the ALLIED [illegible] now ALLIED CORP. at Morristown, USA, is shown in Fig.3. The [illegible] is poured from an induction furnace into a feeder.

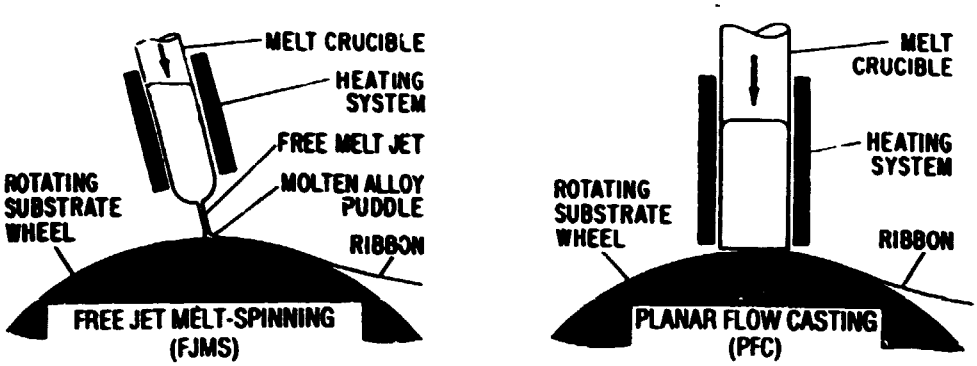

Fig.1. Schematic representation of free jet melt-spinning (FJMS) and planar flow casting (PFC) processes after Liebermann and Bye /9/

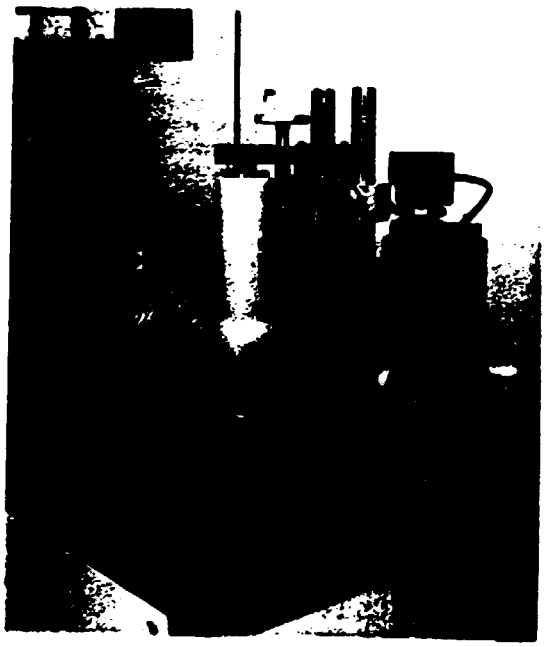

Fig.2. Photo of a laboratory size PFC equipment developed at the Central Research Institute for Physics, Budapest, Hungary

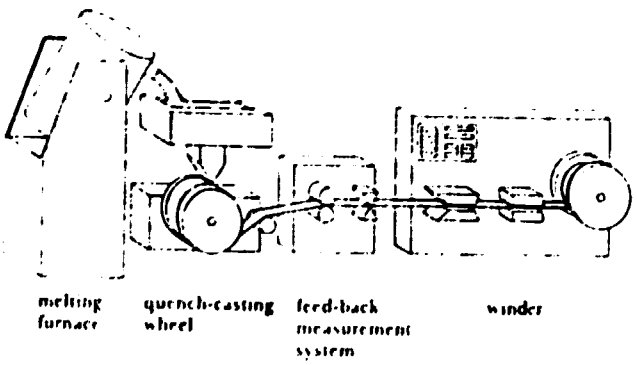

Fig.3. Scheme of a quasi-continuous quench-casting manufacturing line developed by the ALLIED CHEMICAL Corp., Morristown, USA /12/

[illegible] ejected from the nozzle on to the surface of the roller and solidifies into ribbon. It passes through feed-back measurement system then the ribbon is wound up /12/. Another process has been patented by VACUUMSCHMELZE GmbH (Hanau, FRG). The metal is melted in a crucible which has a hole on the bottom. The melt is poured into the nozzle by removing the stopper rod which closes the hole /13/.

For the manufacturing of homogeneous, uniform ribbons a careful control of process parameters is necessary. The influence of manufacturing conditions on the physical properties of the ribbons has been systematically studied for [illegible] of metallic glasses /14-16/, as well as for various microcrystalline alloys /17-19/. The mechanism of ribbon formation itself is the subject of numerous theoretical and experimental studies /8, 20-22/.

Recently, the PFC process is one of the best known and most frequently used methods of rapid solidification. Besides of thin amorphous ribbons (usually 10-50 μm thick), tapes of different microcrystalline alloys (under 1 mm) are manufactured by this method. In some cases the ribbons are precursors for preparing powders by diminution (see sec. 2.3.2).

Among the numerous single-roller processes there are two to be shortly mentioned here. In the melt drag process /23/ the molten metal is fed uniformly across a drum surface to produce a strip of the desired width (Fig.4.). The RIBTECH Company (Gahanna, Ohio, USA) developed the so-called "melt overflow" process for manufacturing ribbons without a nozzle /Fig.5./. This way the procedure was simplified and resulted in a reduction of cost, in particular for narrow ribbons and flakes /24/.

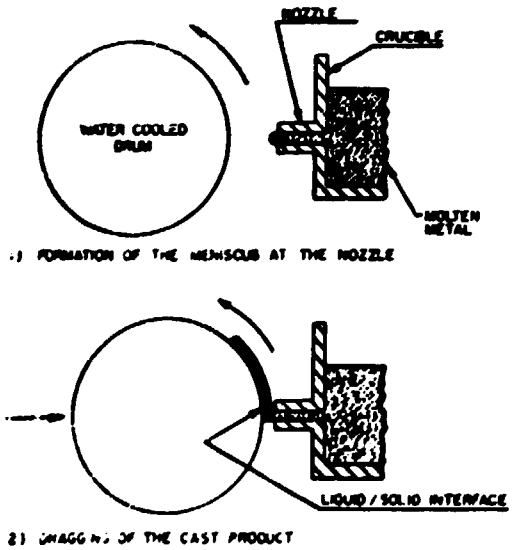

[illegible] principle of the [illegible] process /23/.

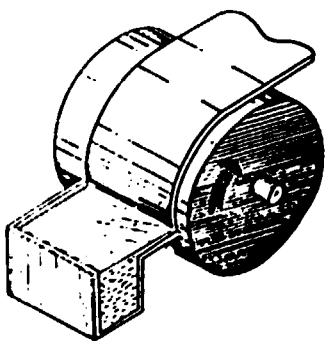

Fig.5. Scheme of RIBTECH's melt overflow process /24/

- twin roller processes: the liquid metal is poured through a nozzle into the gap between two rollers (Fig.6.). This process can be used for producing fine metallic glass ribbons, but the main field of the application is the casting of thicker (from 0.1 to 1-2 mm) sheets of microcrystalline alloys. A commercial size twin roller equipment was described recently by Shibuya and coworkers /25/. The diameter of the water-cooled rollers is 400-500 mm. Fine crystalline strips of Fe-4.5 %Si alloys having 0.2-1 mm thickness and 250-500 mm width have been cast. The charge has been about 500 kg. The solidification rate has been estimated to be about 10^4 K/s.

The present status of the strip casting of ferrous alloys is reviewed by Masumoto /26/. The performance of single roller and twin roller processes have been compared by different authors /27, 28/.

2.2 Preparation of wires

In addition to ribbons, rapidly quenched wires have found practical use, too, for example in certain magnetic sensors or in fiber reinforced composites.

Wires with almost completely circular cross-section and smooth surface have been produced by a modified melt spinning apparatus using rotating water as cooling medium ("in-rotating-water spinning process" INROWASP) /29/. The scheme of the apparatus is shown in Fig.7. The process has been realized on a pilot-plant scale, too. The Japanese firm UNITIKA Ltd (Uji, Japan) developed a method and suitable equipment to mass produce iron-, cobalt-, and nickel-based amorphous wires. The diameter of the wires is in the range of 80-150 μm, the length can be as long as several kilometers /30, 31/. Microcrystalline iron - based /32/ wires have been produced, too. Details on the methods, the role of processing parameters and the properties of the various rapidly solidified wires have been described by several authors /29, 31-33/.

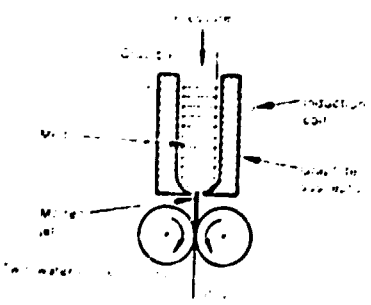

Fig.6. Example for the twin roller technique /8/

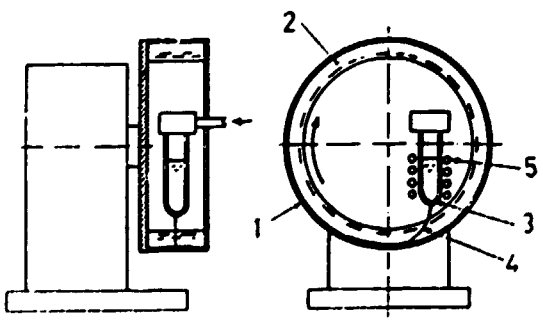

Fig.7. Preparation of wires by the "in-rotating-water spinning process"/29/ 1:rotating drum; 2: liquid coolant; 3:nozzle; 4:melt jet; 5:induction coil

[illegible] amorphous wires by melt extraction [illegible] as [illegible] and Bode /34/. In this techique a rotating [illegible] contact with the melt surface. The extracted metal solidifies into [illegible].

[illegible] Preparation of Powders

The good mechanical properties of rapidly solidified ribbons and wires, [illegible] to their geometry can be exploited for engineering application only in a [illegible] limitation can be partly abolished by the use of the RS [illegible], from which large parts can be produced by the usual powder [illegible] methods. Now the preparation of the RS powders and their consolidation belong to the most quickly developing branches of rapid solidification technologies. The progress is motivated mainly by the demands of aerospace industry for high-strength aluminium alloys.

There is a great number of processes producing RS powders from which the different variants of melt atomization /35, 36/ and diminution (comminution) of RS ribbons /37/ have the greatest practical importance. The status of the production and consolidation of RS powders have been recently summarized by [illegible] /38/, [illegible] and Clive /39/.

[illegible] Atomization. A common feature of the various atomization techiques is the formation of a metal stream, its dispersion to small droplets, and the cooling either by gas or liquid. At the earlier methods the cooling rate was usually not higher than 10^2 K/s, what does not belong to the "rapid cooling" category. As a result of development, the cooling rate has been increased up to [illegible] K/s.

[illegible] In the inert gas atomization processes the stream of molten metal is broken into droplets by a subsonic or supersonic gas jet. The scheme of a [illegible] gas atomization unit is shown in Fig.8. /40/. In most cases Ar, He, [illegible] N_2 gas are used at a pressure of 1-4 MPa. The final products are spherical with satellites. The average particle size can be decreased (and the cooling rate increased) using higher gas velocity. At the OSPREY process the average particle size is between 40 to 50 μm, the velocity of gas stream is about Mach 1, the solidification rate is estimated to be about 10^4 K/s. At the ultrasonic gas atomization at high gas velocity (about Mach 2) higher cooling rates ($10^{[illegible]}$ to $10^{[illegible]}$ K/s) and a smaller average particle size have been reported /38/.

Recently [illegible] et al. described details on ultrasonic gas atomization of [illegible] alloy. The helium gas velocity was about 1700 m/s (Mach [illegible]), the pressure about 6,9 MPa /41/.

In the last years the different methods of spray atomisation and [illegible] rapidly developing (OSPREY process, controlled spray [illegible] dynamic compaction). In these processes the atomized

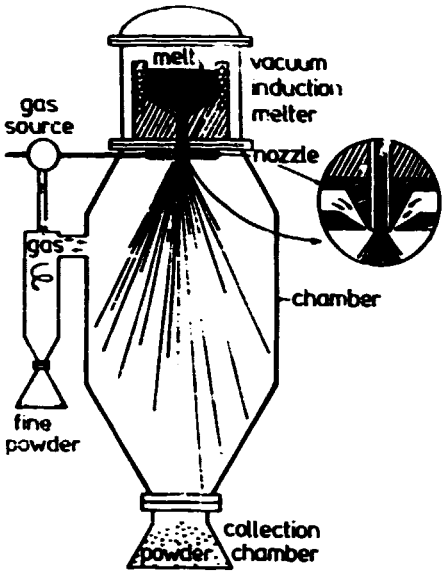

Fig.8. Scheme of a vertical gas atomisation unit as cited by Lawley and Doherty /40/

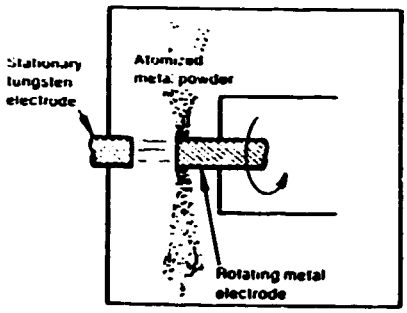

Fig.9. Centrifugal atomisation by the rotating electrode process /38/

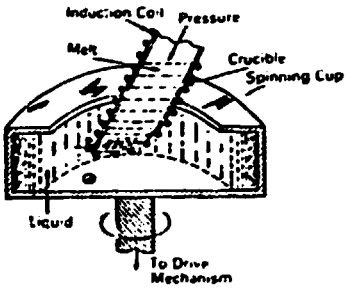

Fig.10. Scheme of the rapid spinning cup apparatus /43/

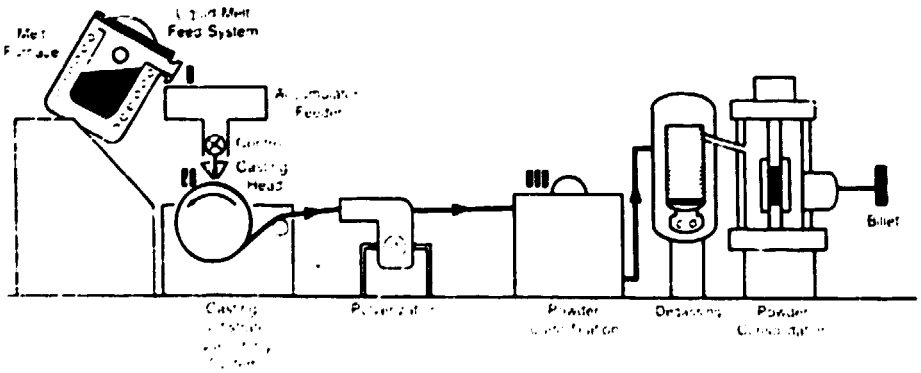

Fig.11. Schematic diagram of a rapid solidification powder process based on planar flow casting-ribbon comminution developed by ALLIED-SIGNAL Inc. /37/

melt droplets are impinged into a shape collector. On impact, the particles flatten and weld together to form a hot, highly dense shaped preform. The formation of refractory oxide films can be significantly reduced by this method /42/.

2.3.1.2 In another class of processes use centrifugal forces are used for atomization. The most important processes are the rotating electrode /Fig. 9./, the rotating cup and the rotating disk methods. High cooling rates (about 10^5 Ks^{-1}) have been reached by the rapid spinning cup process developed at the Battelle Columbus Laboratories (Ohio, USA) /43/. The scheme of the process is shown in Fig.10. Powders under 10 μm in diameter have been produced. This process is now in the laboratory stage but it is very promising for manufacturing of RS powders /44/.

2.3.2 Diminution of RS ribons. The benefits of rapid solidification can be exploited not only by atomization of a melt but by diminution of RS ribbons, too. The later process has many advantages over the atomization: the cooling rate is higher due to the more effective heat removal, the process is less hazardous than the preparation of small sized very reactive particles, the microcellular structure is much more homogeneous and does not depend on particle size, etc. /37/.

Fig.11. shows the schematic diagram of the rapid solidification powder process based on ribbon casting-comminution. It was developed by ALLIED SIGNAL Inc. /Morristown, USA/ to produce aluminium-transition metal microcrystalline powders in tonnage quantities for aerospace application. The particles are typically plates of the order of 100 μm^2 by 25 μm thick /45/.

The diminution of amorphous ribbons plays an imp ortant role in the manufacturing of the newly developed Fe-Nd-B hard magnets. The DELCO REMY, Division of GENERAL MOTORS /Anderson, USA/ has choosen this way instead of the standard powder metallurgical processing /46,47/.

Iron-, nickel- and cobalt based amorphous powders with low metalloid content are produced by diminution of ribbons, too. After heat treatment these alloys become devitrified into multiphase microcrystalline alloys. Additionally, the powders can be fabricated into bulk parts suitable for structural application or into hard wear resistant coatings /48-50/.

2.3.3 Consolidation of RS powders. For the use of the rapidly solidified alloys as structural materials, the production of three dimensionally large shapes is necessary. It can be achieved by consolidation of powders. In addition to common demands of metal powder compaction (high density, chemical homogeneity, near-net-shape), the retaining of RS microstructure/properties is also important.

Several kinds of commercial consolidation processes have been successfully applied recently to RS materials as shown in Table I.

Table I.

Consolidation of RS powders

Method	Alloy	Reference
Hot isostatic pressing	Cu-Ni	/51/
	Cu-Ni-Fe	
Hot extrusion	Fe-B-Si	/52/
	Co-Fe-Ni-Mo-B-Si	
	Al-Mn-Cr	/53/
	Ti-Al-Nb	/54/
Explosive compaction	Ni-P	
	Fe-B-Si	/55/
	Co-Fe-Ni-B-Si	/56/

The status and prospects of the consolidation processes have been critically analyzed by Flinn /38/, Raybold and Cline /39/.

2.4 Surface Melting Processes

If a metal surface is exposed to high energy-density laser, electron or ion beam, a thin rapidly solidified layer can be formed. The process is a special case of substrate quenching, a self-substrate RS method.

A number of excellent review articles covering fundamentals and progress in the development of rapid surface melting has been appeared in the literature /57, 59, 61, 65/.

In practice, the laser surface treatments are especially important /57/. Various types of lasers (CO_2, ruby and Nd:YAG) are used in a wide range of interaction time (from ps to ms). Extreme high cooling rates (10^{10} K/s and more) have been achieved by ns pulsed lasers /58/. Either the beam is scanned or the probe is moved. Common problems are: crack formation in the solidified layer, overlapping of the tracks and the high reflexivity of the metal surfaces. The practical importance of the electron /60/ or ion beam /61/ melting is limited because of the need for vacuum environment.

The surface melting processes are used either for simple melting (glazing) or modification of surface composition (surface alloying and cladding) /59/. Formation of amorphous, as well as microcrystalline surface layers are reported depending on alloy systems and processing conditions. The benefits of rapid solidification (formation of new metastable phases, fine and homogeneously distributed precipitations, grain refinements) are exploited mainly for tool and bearing alloys /62/, cast iron /63/ and various automobile parts /64/.

An alternative to direct surface melting is the plasma spray of RS powders /59, 65/.

The rapid surface melting processes are now mainly in the development stage. Probably, the efforts will lead to a number of practical applications in the near future.

3. AMORPHOUS ALLOYS: PROPERTIES and APPLICATIONS

The metallic glasses (or glassy metals) are rapidly quenched alloys without long range atomic order. In a wider sense, all the non-crystalline (amorphous) alloys are called "metallic glasses", independently of the nature of their formation (e.g. electrodeposition, sputtering, ion implantation etc.).

Their preparation, structure, properties and applications are subject of monographs, conferences (see Appendix I.) and thousands of papers. The most important types of rapid solidification processes has been discussed in Ch.2. In this chapter the properties of metallic glasses are shortly characterized, then the present status of application is reviewed.

3.1 Fundamentals

3.1.1 Atomic structure. Amorphous alloys are frozen liquids with aperiodic structure, /66/ what means that the long range periodicity of the atomic positions is absent. Therefore the structure has to be described by statistical means. The commonly employed description is the atomic pair distribution function (PDF). This microscopic structural quantity can be directly determined by X-ray, neutron or electron diffraction experiments or a combination of them. The PDF describes the probability that two atoms are separated by a distance r:

$$\rho_{AB}(r) = \frac{1}{4\pi r^2 N} \sum_{ij} \delta(r - r_{ij})\, c_i^A\, c_j^B \Big/ c_A\, c_B \quad , \qquad (1)$$

where A, B denote the identity of the atom, C_A C_B denote the composition, N is the total number of atoms, r_{ij} is the separation between the ith and jth atoms and

$$c_i^A = \begin{cases} 1 & \text{if the ith atom is A} \\ 0 & \text{otherwise.} \end{cases} \qquad (2)$$

In alloys, the composition of the nearest neighbours is not necessarily the same as the average composition. The Warren-Cowley parameter α is given by

$$\alpha = 1 - \frac{Z_{AB}}{c_B Z_A} \quad , \qquad (3)$$

where Z_{AB} is the B coordination number around an A atom and Z_A is the total coordination number around an A atom, $Z_A = Z_{AB} + Z_{AA}$ provides the measure of the compositional short range order (CSRO) /67/. If $\alpha < 0$, there is an association tendency of heterogeneous atoms, while if $\alpha > 0$, there is a tendency to dissociation of unlike, or segregation of alike atoms.

a.) Structural models. A series of structural models exists ranging from dense random packing of hard spheres (DRPHS) to "microcrystalline" model. All of them emphasize one or two significant features of the amorphous state as well as their physical properties.

The DRPHS model succesfully describes the high packing density approaching those of crystalline state, what can be achieved in the random structure as well as the average coordination number (12-14). Some of the metal-metal glasses can be characterized well by DRPHS. The DRPHS model was orignally developed for single-component elementary glasses and liquids. In this sense, each atom is a structural unit.

For transition metal-metalloid glasses (TM-M) the "chemically correlated" models are more realistic, because of the covalent bonding character between the constituents is more pronounced /68/. According to these models the structure of glasses is built up from molecular units where the local chemistry dictates the multi-atomic units to be formed (oxide glasses). Similarly to this, TM-M glasses can be regarded as built up from structural units where the local composition is similar to the corresponding intermetallic phase(s). Such structural units could be a consequence of the covalent bonding between TM and M, and also the atomic size ratio between M and TM atoms.

The microcrystalline model is based on the assumption that, since the crystalline state has the lowest energy, the atoms prefer to be crystallized even on a very small scale. In this sense, the amorphous state would be built up from very fine misoriented microcrystalline particles of the appropriate stable or metastable intermetallic compounds.

b. Structural defects and real structure. The oldest concept of a structural defect in the amorphous state is the free volume. The free volume is not homogeneously. Two kinds of regions, the liquid-like regions high in density of free volume and the solid-like regions low in the density of free volume, are developed in

Several structural defects do arise from the preparation circumstances surface crystallization, changing the cooling condition across the cross section of ribbons, etc.) /71/.

5.1.2 Thermal properties. Among the thermal properties the glass-forming ability (GFA) and the thermal stability (glass-crystalline transition temperature, T_{cr}) have a basic importance. Both of them are closely connected with each other. From the details of the GFA one can get information about the nature of the glass-transition, i.e. how the supercooled liquid is vitrified during an appropriate cooling. On the other hand, thermal stability of a glass can be investigated by heating the amorphous material to T_{cr} to produce crystalline phases.

5.1.2.1 Glass transition, glass-forming ability. In Fig. 12. the state functions (enthalpy H, entropy S, and volume V) of a glass-forming system can be seen in various states. In the temperature interval around the T_g glass transition the system quits the thermodynamic equilibrium. This is because the relaxation time, necessary to reach the equilibrium atomic arrangement in the supercooled liquid, will be commensurable with the time of the cooling process as a consequence of the increasing viscosity /72/.

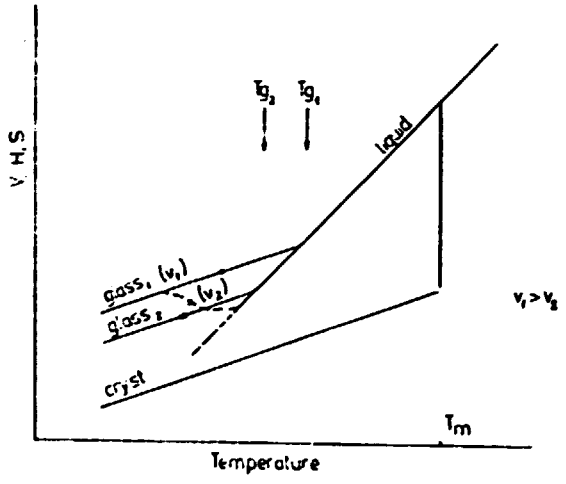

Fig.12. State functions of a glass-forming system in various states /68/. v_1 and v_2 are different cooling rates.

According to Fig.13. the glass-forming ability is the property of a system to solidify without crystallization. In order to vitrify a material, a critical cooling rate R_i^* of the liquid must be exceeded and also a sufficiently low glass temperature (T_g) must be achieved. Both of these are basic criteria of the system. If the necessary cooling rate is less than 10^7 K s^{-1}, the system is regarded as a good glassformer. The supression of the crystallization has a kinetic, as well as a thermodynamic criterion. Between the melting point T_m and T_g, the frequency of the homogeneous nucleation and

The growth of crystalline phases show a very sharp maximum according to

$$I = \frac{K_n}{\eta} \exp\left[-b\alpha^3\beta \Big/ T_r (\Delta T_r)^2\right] \qquad (4)$$

$$U = \frac{K'_n}{\eta}\left\{1 - \exp\left[-\beta \Delta T_r / T_r\right]\right\} \qquad (5)$$

Here K_n and K'_n are kinetic constants, η is the viscosity, b is a shape factor, α and β are dimensionless parameters related to the liquid/crystal interfacial tension σ, and to the entropy of fusion ΔS, $T_r = T/T_m$. From eqs. 4 & 5, follows that the glass formation favours low melting point and high T_g. This is illustrated in Fig.13. From metallurgical point of view the existence of an eutectic point in the equilibrium phase diagram (or at least the large depression of the liquidus temperature) can be regarded as a first criterion for the susceptibility to glass formation. Simultaneously, the existence of stable intermetallic compounds (strong bonding between unlike atoms) and the limited mutual solubility between the components (the non-existence of supersaturated solid solutions) are also necessary for the mass glass formation /73/.

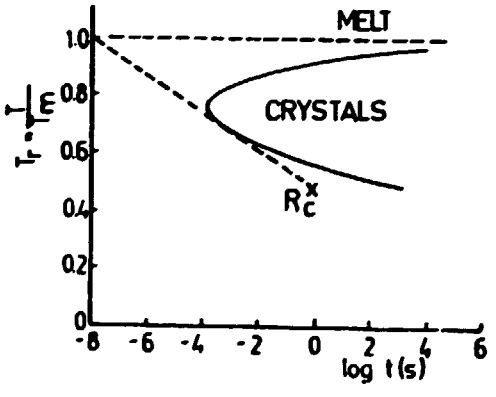

Fig.13. A time-transformation-temperature /TTT/ diagram.

In Table II. some of the well-known glass-forming alloys, together with the appropriate physical constants (necessary for the estimation of GFA) are collected after Davies /74/. From the data it is clear, that the ratio of T_g/T_m can be taken as a guide for estimation of critical cooling rate and for the GFA. Systems with $T_g/T_m \geq 0.4$ are good glass formers.

Table II.

Liquidus T_m and glass transition T_g or crystallization T_x temperatures and predicted critical cooling rates R_c^* for vitrification of some elements and glass forming alloys; R_c^* values based on CCT curves for fraction of crystallization $x = 10^{-6}$; after Davies/74/

Material	T_m K	T_g or T_x K	T_m K	T_g/T_m	R_c^*, K s^{-1}
Ni	1725	(1425)	(1300)	0.25	3.0×10^{10}
$Fe_{75}B_{25}$	1613	(680)	(1025)	0.37	2.6×10^{7}
$Fe_{80}B_{20}$	1569	(680)	(959)	0.40	3.0×10^{7}
Fe	1808	(1280)	(1433)	0.40	3.2×10^{7}
$Au_{49}Ge_{13.5}Si_{13.6}$	639	293	336	0.47	7.4×10^{5}
$Fe_{81}B_{19}$	1448	760	688	0.52	1.0×10^{6}
$Fe_{81}Ni_{81}B_{19}$	1352	720	632	0.53	3.5×10^{5}
$Co_{80}Si_{12}B_{10}$	1393	785	608	0.56	3.5×10^{5}
Co	1210	(750)	(1460)	0.62	5.0×10^{5}
$Fe_{40}Ni_{40}B_{20}$	1449	818	601	0.58	1.8×10^{5}
$Ni_{75}Si_8B_{17}$	1340	782	558	0.58	1.1×10^{5}
$Fe_{80}P_{13}C_7$	1258	736	522	0.59	2.8×10^{4}
$Pt_{60}Ni_{15}P_{25}$	925	500	375	0.57	4.0×10^{3}
$Pd_{80}Si_{20}$	1071	657	414	0.61	1.8×10^{3}
$Ni_{62}Nb_{38}$	1442	945	497	0.66	1.4×10^{3}
$Pd_{77.5}Cu_6Si_{16.5}$	1015	653	362	0.64	3.2×10^{2}
$Pd_{82}Si_{18}P_{20}$	916	602	314	0.66	1.2×10^{2}

On the basis of the chemical character of the constituent elements, the glass-forming alloys can be categorized into the next groups:

a.) Metal metalloid systems /TM-M/: e.g. Fe-B, Ni-B, $(Fe,Ni,Co)_{80}(P,B,C)_{20}$

b.) Metal metal systems:

late-early transition metals, e.g. Ni-Nb, Ta-Ir, (Co,Ni,Cu)-Zr

metal-transition metal, e.g. Be-Ti, Be-Zr

transition metal -rare earths, e.g. Co-Sm, Ni-Gd

transition metal-actinides, e.g. U-V, U-Cr.

5.1.2.2 Thermal stability. The thermal stability may be characterized by the temperature at the onset of the crystallization. The crystallization temperature T_{cr}, similarly to T_g, depends mainly on the bonding state in the glass. The bonding state determines the atomic diffusion which results in crystallization.

[illegible] also depends on the type of the crystallization process, whether it is primary, eutectic or polimorphous. The type of crystallization beginning with primary nucleation and crystal growth is activated more easily than the eutectic one where the surface energy has an important role /5/. At a given type of crystallization reaction both T_g and T_{cr} are the intrinsic property of the constituent elements. As a consequence of this, the thermal stability (T_{cr}) changes systematically with the properties of the constituent metals in the periodic system (together with other physical properties), as it was pointed out by several investigators /6, 77/. A typical example, Fig.14. shows the systematic change of T_{cr} with microhardness (HV) in Co-, Ni-, and Fe-based glasses if the host metal is partially replaced with other metallic elements.

The values of T_{cr} have been collected for several alloys in Table II. Thermal stability data on amorphous binary alloys can be found in a review article by Wang /78/.

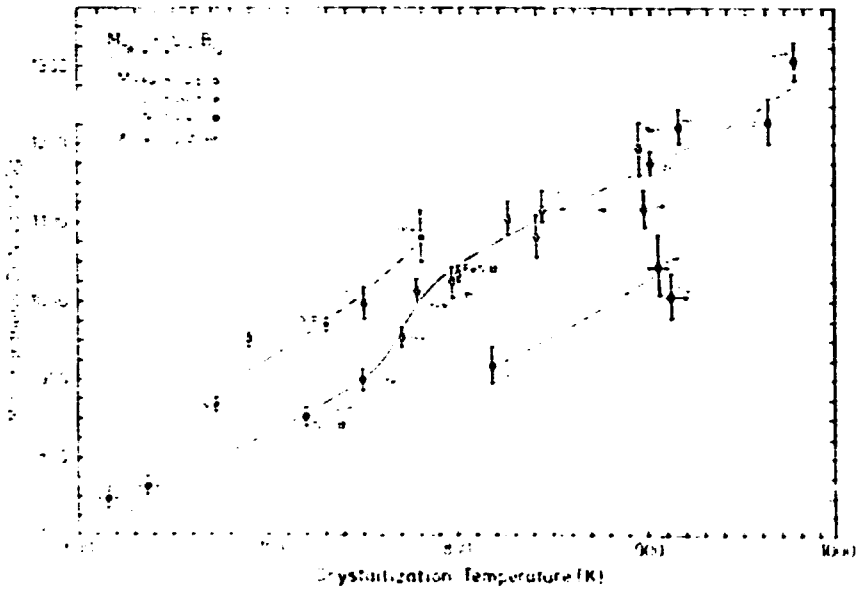

Fig.14. Microhardness of Fe-and Ni-based glassy alloys as a function of crystallization temperature /76/

5.1.3 Structural relaxation. Amorphous alloys in the as-prepared condition are not only metastable with respect to the appropriate crystalline phase(s), but also unstable with respect to a differently configurated, denser amorphous state. Atomic rearrangements within the glass state gradually lead towards this "ideal" amorphous structure. The sum of these atomic-scale rearrangements is called structural relaxation. The description of the kinetics of the relaxation involves the use of a spectrum of relaxation times and a spectrum of activation energies /79/. Most of the properties display a combination of reversible and irreversible structural relaxation. For a given material some properties may show a large reversible component and others a negligible one.

5.1.4 Physical properties. a.) Electronic structure. According to the data of photoemission experiments, there is a strong similarity between the liquid

and glassy states. On the other hand essentially the same d-band peak positions were found for several transition metal-transition metal glasses and in the corresponding crystalline state. This means that alloying determines predominantly the electronic structure, and the order-disorder is only of secondary importance.

3.1.4 Electrical resistivity of glassy alloys is relatively high, ranging from 50-400 $\mu\Omega$cm and it is weakly temperature dependent. The temperature coefficient, α, however, can be either positive or negative, depending on the composition. Among the attempts to explain this behaviour, the Ziman-Faber theory (originally introduced to explain the resistivity of simple liquid metals) appears to be most consistent with the experimental results.

3.1.5 Magnetic properties. The saturation magnetic moment (μ) of 3d transition-metal based amorphous alloys as a function of the nominal d-electron concentration, n_d follows a curve similar to the Slater-Pauling curve for crystalline alloys (Fig.15.). Compared to the Slater-Pauling curve of crystalline alloys, the curves for amorphous alloys are shifted towards smaller values of n_d. Similar behaviour was observed for crystalline compounds such as $(Fe\text{-}Co\text{-}Ni)_2B$. This shift is due to the metalloid element reducing the moment of transition metal. Similarly the Curie temperatures for amorphous alloys are generally lower than those of pure transition metal alloys of the same composition.(Fig.16.) /80/.

The effective permeability (μ_e) has been measured for a variety of alloys prepared under different conditions. The value of μ_e reflects the anisotropies developed: namely the shape and strain anisotropy and the field or stress-induced anisotropy. The contribution of these sources is widely investigated /81/. The permeability in the as-quenched state is low, except in $\lambda \approx 0$ compositions. Fig.17. shows the main role of the magnetostrictive anisotropy determining the value .

The main sources of coercivity H_c of amorphous ribbons consist of the following contributions: intrinsic fluctuations of the exchange and of the local anisotropy, clustering of atoms due to short range ordering, surface irregularities and volume pinning effects. H_c is decreased by the structural relaxation.

The value of the magnetostriction coefficient of ferromagnetic glassy alloys covers a wide range from about 40×10^{-6}, through zero to -4×10^{-6}.

The power loss in the amorphous state is frequently less than in the crystalline one. Similarly to the crystalline magnetic alloys it can be divided into three parts: namely static hysteresis loss, classical and excess (eddy current losses). Fig.18.). From experimental measurements it has been shown, that the excess eddy current loss is responsible for 90-99 % of the total power loss of the amorphous materials. The progress in the study of amorphous magnetism has been reviewed recently by O'Handley /82/.

3.1.6 Mechanical properties. Mechanical properties constitute the most unique

Fig. ... Slater-Pauling curve of TM-M alloys after O'Handley /80/

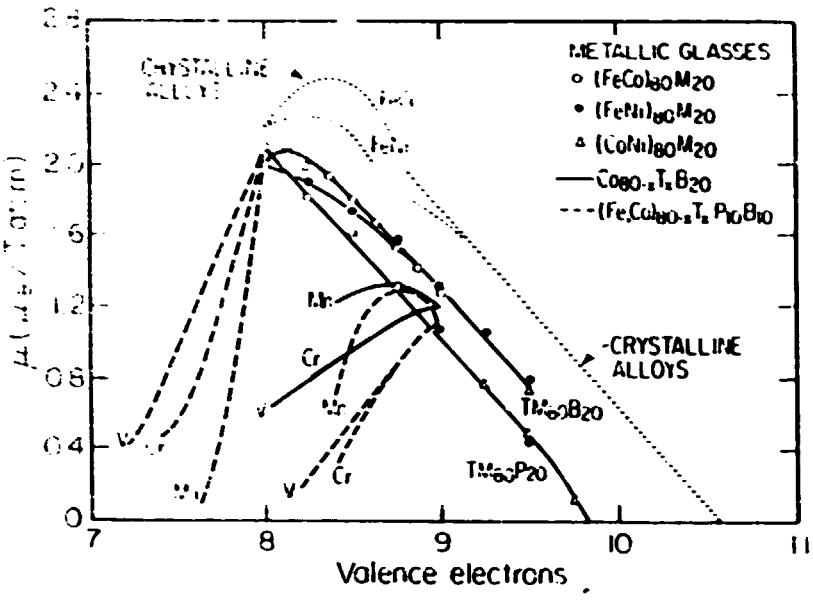

Fig.16. Curie temperatures for various $T_{80}P_{10}B_{10}$ amorphous thin films after O'Handley /80/

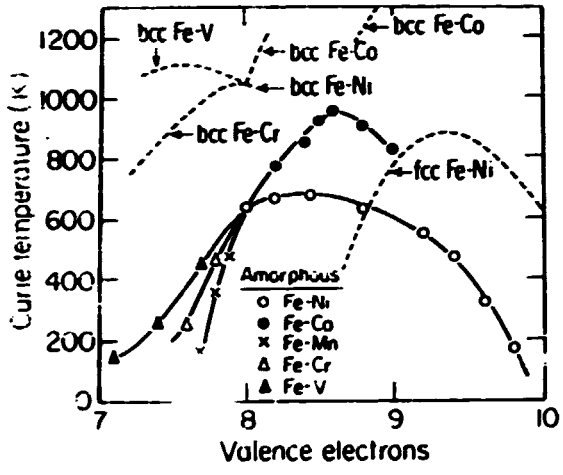

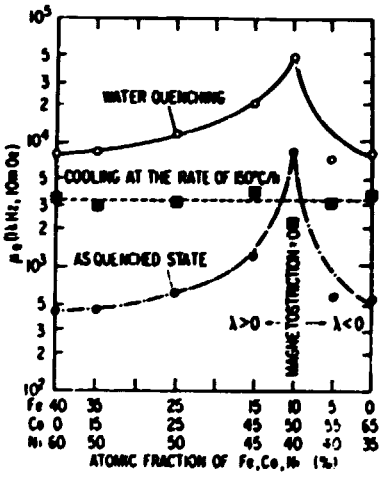

Fig.17. Permeability measured at 1 kHz and 10 mOe of various $(Fe,Co,Ni)_{78}Si_8B_{14}$ alloys with T_c near 300°C after O'Handley /80/ as quenched, water quenched from 450°C or slowly cooled from 450°C

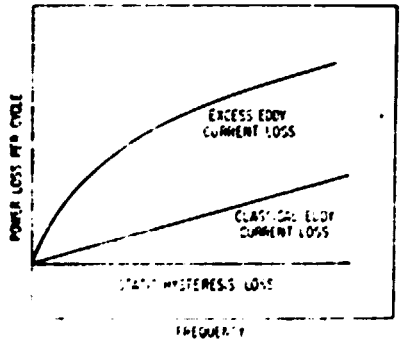

Fig.18. Classical separation of ... as a function ... frequency, into its ... components /80/

characteristics of glassy alloys. Fracture in these alloys proceeds by highly localized shear deformations in contrast to the brittle fracture, commonly observed in non-metallic glasses. Because of the lack of translational periodicity, the fracture strength of glassy metals approaches the theoretical strength / $\sigma_F \sim \frac{E}{50}$ / as compared with $\sigma_F \sim \frac{E}{10^3}$ to $\sigma_F \sim \frac{E}{10^2}$ observed for crystalline metals where dislocations are created and propagate through the crystalline lattice.

Metallic glasses exhibit an interesting combination of mechanical properties, a very high fracture strength and high fracture toughness. The ductility and thoughness of Fe-based glasses are very susceptible to thermal annealing and hydrogen enviroment. A complete loss in ductility of Fe glasses may occur after annealing without crystallization.

The fracture strength σ_f , hardness H , Young's modulus E , Poisson's ratio ν and fracture tensile strain ϵ_f (10^{-2}) of some typical glassy metals are listed in Table.III /68/.

Table III.

Fracture strength of glassy metals. Vicker's hardness H (kg mm^{-2}), fracture strength σ_f (kg mm^{-2}), Young's modulus (10^3 kg mm^{-2}), Poisson's ratio ν and tensile yield strain ϵ_y (10^{-2}).

	H	σ_f	H/σ_f	E	ν	$\epsilon_y = H/3E$
$Pd_{77.5}Cu_6Si_{16.5}$	485	157	2·91	9·3	0·41	1·52
$Pt_{57.5}Ni_{14.7}P_{27.8}$	452	160	2·83	9·4	0·39	1·50
$Pd_{40}Ni_{40}P_{20}$	541	150	3·01	10·6	0·40	1·74
$Fe_{80}P_{20}$	548	-	-	9·3	0·43	1·23
$Co_{75}B_{25}$	1155	—	—	18·0	0·34	2·15
$Fe_{75}B_{25}$	1314	—	—	17·9	0·32	2·45
$Ni_{75}Si_{25}$	893	—	—	13·2	0·37	2·26
$Zr_{76}Cu_{24}$	530	—	—	8·5	0·36	2·27
$Ti_{76}Cu_{24}$	610	—	—	10·0	0·36	2·06

Fe-based glasses are very sensitive to quenching conditions /16/ and tend to be brittle, whereas glass-forming Ni, Pd and Pt alloys exhibit a high ductility even in a partially crystalline state.

5.1.7 Chemical properties. Amorphous alloys containing significant amounts /> 5%/ of Cr show excellent corrosion resistance both in concentrated acid and in electrolitic solutions /84/. The resistance is due to the formation of a dense oxo-hydroxide layer on the metal surface. Unlike the crystalline metallic surfaces the protective layer would not be broken by the grain boundaries, resulting in a much better corrosion resistance. The corrosion resistance however, is not at all a general property of the amorphous alloys. Al-, or without Ti or Mo are susceptible to environmental attack.

The amorphous alloy surface was found to have a good catalytic potential [85, 86].

3.2. Application of Metallic Glasses

The unusual properties of metallic glasses have been exploited since 1976 when ALLIED CHEMICAL CORPORATION (now Allied Corporation) introduced flexible magnetic shields to market. The soft magnetic glassy metals represent till now the most important field of application. Among the other products the brazing foils and amorphous fiber reinforcement materials have been widely disseminated. A number of devices and materials are in the stage of development. Comprehensive articles on application of metallic glasses are available in the literature /3, 12, 62, 89/.

3.2.1 Soft magnetic materials. The special atomic arrengement, the isotropic character, the absence of grain boundaries result in such properties and property combinations which are favourable for practical applications. The most remarkable ones are as follows: high permeability, low coercivity (narrow B-H loop, good core properties), good domain-wall mobility (ease of magnetization), high ΔE effect, high electrical resistivity, thickness (good high frequency behaviour). These properties are frequently coupled with high mechanical hardness and with good corrosion resistance. Additionally, the glassy structure makes possible a wider choice of alloy compositions than in the case of the microcrystalline ones. It means that the composition (and processing) can easily be taylored to various requirements, e.g. positive, negative or zero magnetostriction coefficient; flat or rectangular shaped B-H loops, etc.

The fundamental aspects of amorphous magnetism /82/, guides for material selection /89/, the most important fields of soft magnetic applications /90-93/, and the problems of commercialization /94-96/ have been summarized recently in numerous review articles.

Based on developments during the last decade, the compositions of the most promising types of soft magnetic glassy metals have been established /97/, namely:

a.) iron based alloys with high (1,6-1,8 T) saturation magnetization, relative low permeability and high magnetostriction coefficient. These were originally developed for distribution transformer applications but they can be used at higher frequencies (about up to 50 kHz), too.

b.) cobalt based alloys with lower saturation induction (0,6-0,9 T) but with excellent high-frequency properties (up to about 500 kHz) and nearly zero magnetostriction.

Typical alloy compositions and related magnetic properties are shown in Table IV. following /97/.

Table IV.

Properties of Some Amorphous Magnetic Alloys (From C. H. Smith, Ref/97/ Table I)

Alloy	B_s (T)	H_c (A/m)	λ_s (10^{-6})	ρ ($\mu\Omega$cm)	T_x (°C)	Core Loss 60 Hz, 1.4T (W/kg)	Core Loss 20 kHz, 0.2T (mW/cm^3)
Fe-based							
$Fe_{81}B_{13.5}Si_{3.5}C_2$	1.61	3.2	30	130	370	0.3	300
$Fe_{78}B_{13}Si_9$	1.56	2.4	27	130	415	0.23	-
$Fe_{77.5}Si_{7.5}B_{15}$	1.50	4.0	35	130	415	0.35	-
$Fe_{40}Ni_{40}P_{14}B_6$	1.55	8.0	27	125	405	1.2	35
Fe-Ni-based							
$Fe_{39}Ni_{39}Mo_2Si_6B_{14}$	0.55	1.2	12	160	353	-	200
Co-based							
$Co_{66}Fe_4Ni_1Mo_2B_{16}Si_{11}$	0.72	0.4	0.3	135	340	-	43

Soft magnetic amorphous materials are now commercially available both as ribbons and components (e.g. induction coils, transformers, recording heads). The amorphous magnetic wires and powders are in the stage of development. A list of manufacturers and products is compiled in Appendix II.

3.2.1.1 Transformers. For many years the driving force for the development of metallic glasses was the saving of energy in distribution transformers /98/. The advantages of amorphous cores can be seen in Fig.19. where core loss data are given for prototypes of transformers made by different manufacturers and in different sizes /12/.

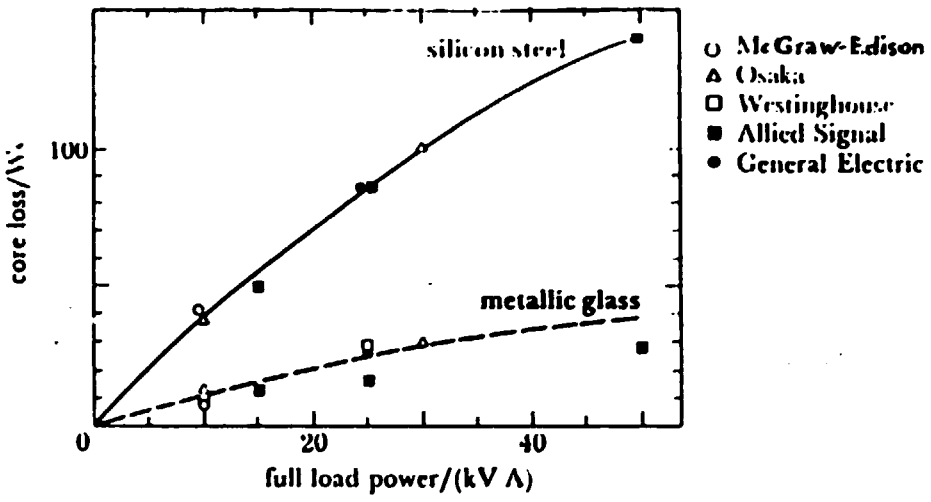

Fig.19. Energy losses in transformers of various sizes made by various companies after Gilman /12/

Iron based amorphous ribbons, very frequently ALLIED Corporations' METGLAS® 2605 S-2 alloys /99/ are used in this types of transformers. Various technical problems arise by substituting the polycrystalline Fe-Si sheets for metallic glasses. These problems are due to the mechanical

hardness, the embrittlement after annealing, the unusual thickness and the high magnetostriction coefficient. Therefore a new transformer design is necessary /100, 101/. In several countries manufacturers have managed to solve these problems /e.g. GENERAL ELECTRIC, WESTINGHOUSE in the USA, OSAKA and TAKAOKA in Japan, HYDRO-QUEBEC in Canada/. To provide a thicker product ALLIED CORPORATION developed a technique for laminating strips by warm consolidation for use in stacked core transformers. These POWERCORE^{R} strips are up to 10 layers thick and have a packing fraction better than that of a single wound ribbon core /102, 103/.

The most intensive development work on amorphous core distribution transformers is carried out in the USA, Canada and Japan where the field performance of these devices is studied in the framework of large-scale projects. In the USA the Electric Power Research Institute (EPRI) and the Empire State Electric Energy Research Corporation (ESEER), in cooperation with manufacturers organized a standard test program. After nearly two years of continuous operation no significant change in power loss was found /104, 105/.

Recently ALLIED-SIGNAL announced plans to construct a 60.000 ton/year capacity facility to produce METGLAS^{R} amorphous ribbons for these applications /89/. The installation of a production line for distribution transformers has been completed by WESTINGHOUSE ELECTRIC Corporation /103/.

Amorphous ribbons have found practical use in several other types of transformers, including 400 Hz power transformers in airborne and military applications /87/, and large pulse transformers used e.g. in linear accelerators /106/.

5.2.1.2 Inductive components for electronics. There is a rapidly growing interest in the application of metallic glasses as special transformers and induction coils in different branches of electronics /89, 92, 107, 108/. Appropriate choice of composition and subsequent heat treatment of ribbons enable the magnetic properties of these devices to be tailored to meet widely differing requirements.

One of the most important field of application is the switched-mode power supplies operating at 10 kHz to 200 kHz, where the metallic glasses can replace the conventional soft magnetic materials in inverter transformers, saturable core reactors, current compensated chokes and spike killers /109/. A number of inductive components for these application have been commercially available since the early eighties /110, 111/.

Amorphous ribbons can be used instead of permalloy or supermalloy in earth leakage circuit breakers (ground fault interrupter). The main part of these devices consists of a toroidal core operating as a differential current transformer. Zhang reported the use of Co-based alloys for small fault currents and Fe-Ni-V-Si-B glasses for large ones /107/. ALLIED CORPORATION developed cheap, iron based metallic glasses (METGLAS^{R} 2605 SM and 2605 S-3)

for these purposes /112/.

5.2.1.3 Magnetic heads. The combination of good soft magnetic properties and high wear resistance gave a good possibility to use metallic glasses in various magnetic heads for audio, video and data storage applications.

Cobalt based, nearly zero magnetostriction alloys meet the demands for attaining high density, high frequency and high reproducibility recording. Many details have been published on the magnetic properties of amorphous alloys and on the design of amorphous magnetic heads /113/.

Amorphous magnetic heads are commercially available since 1981. Audio heads are manufactured at a rate of more than three millions per year by Japanese firms TDK Co., MATSUSHITA Co. SONY Co. and others /92/. Video tape recorder heads are produced in Japan and in Europe /113-115/. Amorphous heads for data storage applications are also available /113, 116/. In many cases microcrystalline Fe-Si-Al ribbons are used for the same purposes (see section 4.2.3).

5.2.1.4 Magnetic shields. Metallic glasses having high permeability and low magnetostriction can be used for magnetic shielding /117/. As it has been mentioned, ALLIED's flexible magnetic shields (under trademark METSHIELD^{TM}) were the first commercial amorphous metal products /97/. A number of applications make use of glassy metal magnetic shields e.g. spiral wrapped cable shielding /118/, and shielding of cathode ray or TV tubes /119/.

5.2.1.5 Sensors and transducers. Currently, the interest is rapidly growing towards different types of sensors for mechatronics, robotics and other branches of industry. High sensitivity, independence on environment (temperature, humidity), robustness, small size: these are only a few of the strict requirements against these devices. The special magnetostrictive behaviour (either very low or very high magnetostriction coefficient), high magneto-mechanical coupling factor (ΔE effect), the high tensile stress, simultaneously with good soft magnetic properties and corrosion resistance, combine to make the metallic glasses possible candidates for sensor materials /90/. Several types of amorphous sensors are already commercially available but the majority of them are still in the development. The principle and the practical use of amorphous sensors have been summarized by Mohri /120, 121/.

5.2.2 Brazing filler materials. Among the non-magnetic applications first of all the ductile amorphous and microcrystalline brazing filler alloys are worth mentioning. They have been developed by ALLIED CHEMICAL CORPORATION at the end of the seventies /122, 123/.

The MBF brazing foils have many advantages over the traditional ones: they are chemically more homogeneous, do not need any organic binder and have excellent wetting characteristics. The form of ribbon instead of powder-binder composites makes the handling easier.

Recently, the ALLIED CORPORATION offers different types of ductile brazing foils including nickel based alloys for high temperature brazing

(e.g. Ni-P, Ni-B-Si, Ni-Cr-Fe-B-Si, Ni-Pd alloys) as well as aluminium or copper based alloys for lower temperature brazing and soldering /124, 125/.

5.2.3 Fiber reinforcement materials. Both the good mechanical properties and corrosion resistance of amorphous alloys are exploited in the use of wires or ribbons for fiber reinforcement in concrete. Relative short (15-25 mm long) wires or narrow ribbons (0,5-1,0 mm) are added to the concrete in 1-2 volume % /126/. This technique is important in the manufacturing of thin surface layers or shell type constructions of concrete. Good results are reported recently by Magyari in the testing of a 30 mm thick shell structure /127/.

5.2.4 Catalysts. The use of amorphous alloys as special, selective catalysts are now in the stage of development. The recent results are encouraging /85, 86, 128/.

6. RAPIDLY SOLIDIFIED CRYSTALLINE ALLOYS

Since the second half of the seventies the microcrystalline alloys have received a growing interest. With respect to processing, one distinguishes two major groups: alloys prepared by rapid solidification of metallic melts, and alloys made by devitrification of amorphous precursors.

In both cases, the advantages of rapid solidification are utilized: the extension of solubility limits, the formation of new, metastable phases and refinements of grain size. These features result in improved properties as higher ultimate tensile and yield stresses, better elongation, good corrosion resistance, etc.

The majority of microcrystalline alloys is prepared nowadays by rapid solidification processing using the methods discussed earlier (Ch.2). The microstructural features (e.g. dendrite arms spacings, grain size) can be influenced greatly by the solidification rate /Fig.20/. The typical grain size is between 1-10 μm. First of all, the high performance structural alloys, special soft magnetic alloys, and some type of brazing filler materials belong to this category.
In other cases the crystallization of amorphous ribbons (devitrification) is used to form a microcrystalline structure. Iron- and nickel-based structural materials and iron-neodymium-boron hard magnets have been produced by this way.

In this chapter, first a short introduction to rapid solidification phenomena is given, then the major fields of applications are discussed. For a detailed treatment we refer to the literature, especially to proceedings of conferences and symposia organized on these topics (see Appendix 1.).

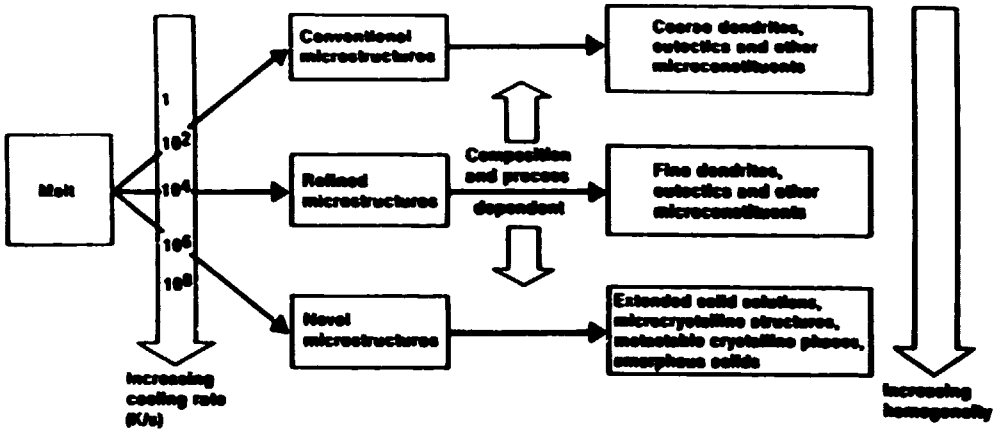

Fig.20. Microstructural consequences of rapid solidification after Flinn /38/

4.1 Constitutional and Microstructural Features of Rapidly Solidified Alloys

The solidification of an alloy from the melt can lead to various microstructural features depending on the following parameters:

- alloy-composition,
- temperature gradient in the liquid just ahead of the advancing liquid/solid interface /G/,
- interface velocity or solidification rate /R/,
- surface energy of the solid/liquid interface,
- impurity types and levels in the melt,
- growth mechanism of the solid phases.

The purpose of this chapter is to give a short overview of the microstructural consequences of the applied cooling rate /1, 129-131/.

The microstructural consequences of rapid cooling from melt are summarized in Fig.21 the (cooling rate $\dot{T}$ is defined as the product of the temperature gradient G and solidification rate R). In passing from ordinary casting practice to cooling rates greater than 10^2 K/s, the microstructural features become refined because the time for coarsening during solidification is reduced. With still higher cooling rates, however, nucleation can be depressed to temperatures well below the liquidus temperature, and novel microstructures come into existence (extended solid solutions, metastable phases /38, 132/).

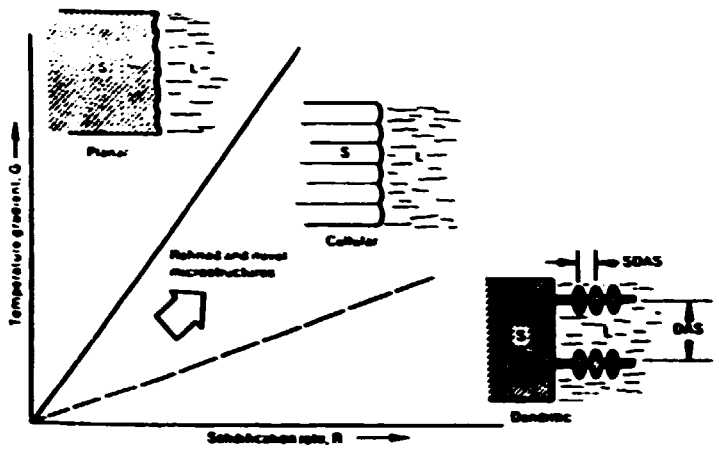

Fig.21. Scheme showing morphological developments from rapid solidification after Flinn /38/
DAS: dendrite arm spacing,
SDAS: secondary dendrite arm spacing

From the point of view of the development of the microstructure, the distribution of solute atoms between the solid and solidifying melt, as well as the morphology of solid/liquid interface have a basic importance. Both of them can be treated quantitatively on the basis of the fulfilment of equilibrium conditions at the solid/liquid interface (or the degree of the departure from it). Consequently, we can classify the events at the interface, and also the resulting microstructural features as a function of "the hierarchy" of equilibrium states /1, 133/

a.) The full diffusional (global) equilibrium (in which the equilibrium is maintained at all time) never fulfills in the practical cooling processes. This can happen only if the rate of the advancing of the interface is slow compared with the diffusion rate of the relevant solute in the solid, and if the required diffusion distance is small. As a result, there is no chemical potential gradient, and the composition of the solid and liquid is the same.

b.) In all practical cases the equilibrium is maintained only at the interface, and the local composition of the solid or liquid at the interface differs from the average ones. If the interface velocity is slow (cooling rate 10^{-6}-10^{-3} K/s) and the temperature gradient is high, a planar interface morphology develops /Fig. 21/, and

$$k = \frac{C_s}{C_l} \qquad (6)$$

fulfils at the interface, where C_s and C_l are the equilibrium interface compositions, being fixed by the phase diagram, and k is the equilibrium partition ratio. One must emphasize that k is different from unity (usually less than 1) as a consequence of the different thermodynamic activity of the solute atoms in the liquid and solid phases. As the solidification proceeds,

the solute is rejected into the liquid. The diffusion in the liquid is usually limited, so a solute-enriched boundary layer builds up ahead of the advancing interface (see Fig.22). The concentration of the liquid at a distance x' from the interface can be expressed as:

$$C_l = C_o \left(1 + \frac{1-K}{K} e^{-\left(R/D_L\right)x'} \right) \qquad (7)$$

where D_i is the diffusion coefficient of the solute in the liquid, C_o is the overall alloy composition.

From Eq.7 it is clear, that D_L/R may be considered as a characteristic distance determining the width of the boundary layer. With increasing speed rate of the solidification front the solute distribution curve will be steeper (Fig.23), what means that the available time is not enough to build up the steady state form of the boundary layer, so the value of partition coefficient will vary in this case according to /134/

$$K^x(R) = \frac{K + \beta_o R}{1 + \beta_o R} \qquad (8)$$

($\beta_o = \frac{2l}{D_L}$, where l is the atomic distance).

This interaction (between R the solid front and the boundary layer) is the source of perturbations, responsible for the constitutional supercooling (CSC) and it leads to the destabilization of the planar interface.

The condition of the CSC is:

$$G \leq \frac{mR}{D} C_s \frac{1-K}{K}$$

where m is the slope of the liquidus line).

c.) In the range of cooling rates $R_{cs} < R < R_{ab}$ (where R_{cs} is the critical velocity for the introduction of CSC, R_{ab} the critical velocity for absolute stability the constitutional supercooling is predominant in the cooling system. The appropriate microstructural manifestation is the appearance of dendrites and cellulars in the solidified structure.

The dendritic structure shows a continuous refinement as the applied cooling rate increases, which is characterized empirically by a power law: 135

$$\lambda = B \epsilon^{-m} \qquad (9)$$

where B const, $\epsilon = G.R$ cooling rate.

In this way the dendritic arm spacing λ /Fig.24/, and eutectic interlamellar spacing Λ /Fig.25/ can be regarded as a measure of the cooling rate for a given system.

d. In the range of 10^5 K/s cooling rate the stable phases cannot always separate out from sufficiently fast, therefore the local compositional

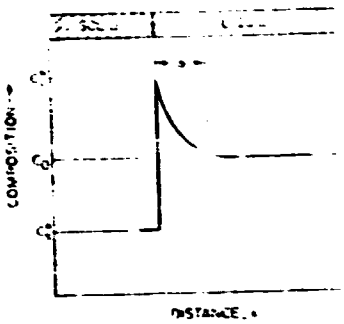

Fig.22 Solute profile in the liqu for solidification with con vection

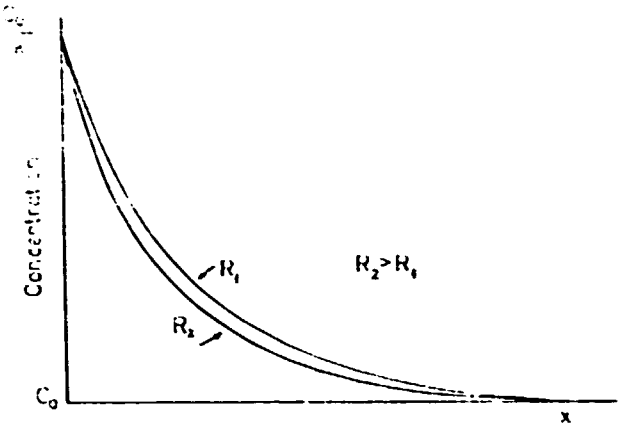

Fig.23. Solute distribution in melt under various solidification rate /R/

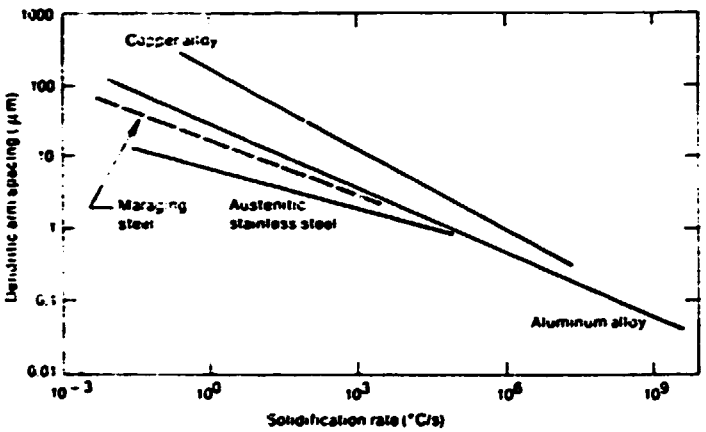

Fig.24. Dendrite arm spacing versus solidification rate for aluminium and copper alloys and two steels after Flinn /38/

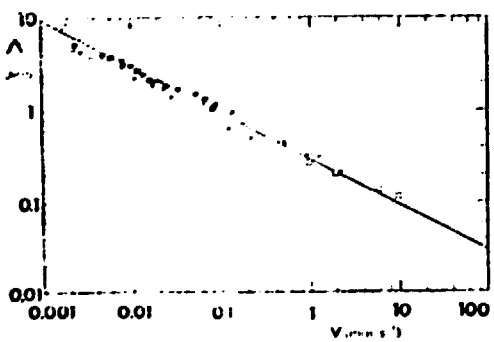

Fig.25 Eutectic interlamellar spacing Λ as a function of growth velocity, for Al-Al_2Cu eutectic plotted by Jones /62/

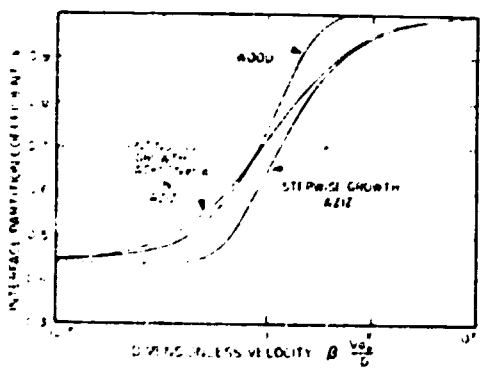

Fig.26. Curves showing the dependence of the interface partition coefficient k on velocity /134/

circumstances at the solid/liquid interface favour the formation of metastable phases, and the metastable phase-relations determine the interface conditions. According to Eq.8, it is clear that the partition coefficient is velocity dependent and changes from k (its equilibrium value) to unity as the growth velocity increases /Fig.26/. As k approaches unity, more and more solute atoms are trapped by the rapidly moving interface and k=1 is the kinetic condition for partitionless formation of single phase extended solid solutions, based on the terminal phase of an alloy system /136-138/.

The kinetical picture of the solute trapping is, that, while solvent atoms can be transferred from the liquid to the solid by making only small shifts in position and bonding, the solute atoms would need to diffuse over long distances to avoid being engulfed by the rapidly moving solidification front.

The thermodynamic criterion for the solute trapping is the possibility of the undercooling below the T_0 curve, where the molar free energies of the liquid and solid phases are equal /139/.

The geometrical structure of T_0 curves is illustrated in Fig.27 for two different eutectic phase diagrams. This curve is very important in determining whether a boundary exists for the extension of solubility by rapid cooling. If the T_0 curves plunge to very low temperatures, as seen in Fig.27a, single phase crystals with composition beyond their respective T_0 curves cannot be formed from the melt. Such systems are susceptible to the amorphous phase formation. In this range of the freezing velocities (10^5-10^{10} K/s) either solute trapping or a glass transition occurs. There is only a limited time available, so any lateral solute segregation in the liquid can only take place for perturbations of the solid-liquid interface having very short wave-lengths. These short wavelengths require such a large increase in the area of the interface that the perturbations are retarded by capillary forces and the planar interface is stabilized again. Therefore the resulting phase is "featureless".

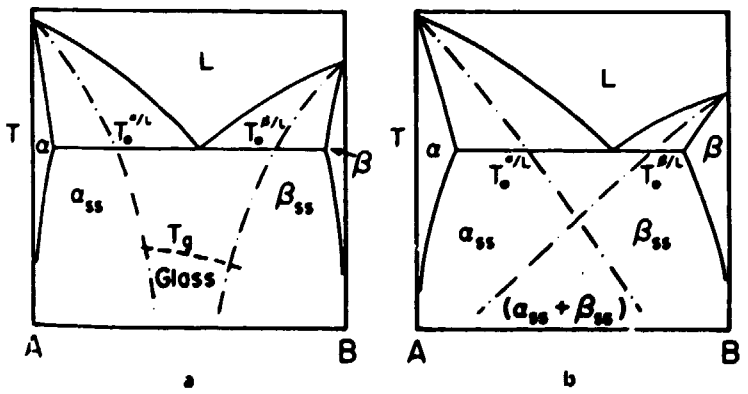

Fig.27. Schematic representation of T_0 curves for the liquid to crystal transformation in two types of eutectic systems as cited by Boettinger and Perepezko /133/

4.2 Application of RS Crystalline Alloys

4.2.1 High performance structural materials. The development of high performance structural materials was recently motivated by the requirements of the aerospace industry. A number of aluminium-, magnesium- and titanium based rapidly solidified alloys proved to have better mechanical and corrosion properties than the conventional wrought ingot alloys.

Aluminium alloys. It is known that the equilibrium solid state solubility (and the diffusivity) of transition metals in aluminium is very low. Only about eight alloying elements have higher solubility than 1 at.% /3/. The rapid solidification in many cases extended the solubility and it made possible a wider range of compositions to be chosen.

Three types of alloys are in the focus of the interest: high strength corrosion resistance alloys (7 XXX and 2 XXX series), low density alloys (Al-Li based) and high temperature alloys (Al-Cu-transition metal alloys) /3, p. 69, 140-143/.

The precipitation hardened Al-Cu-Zn-Mg-Co type alloys belong to the first group (e.g. 7090 and 7091). These are commercially produced by atomization at several manufacturers in the USA (ALCOA, KAISER). The 10^4 °C/s cooling rate results in secondary dendrite arm spacings ranging from 1 to 5 μm. The content of the alloying elements is increased compared to usual compositions /42, 143/.

The second group of alloys has a low density and a high elastic modulus (Al-Li-X alloys). Each weight percent lithium added to aluminium can increase the elastic modulus by six percent and decrease the density by three percent. Recently ALLIED-SIGNAL Inc. developed two types of rapidly solidified Al-Li-Cu-Mg-Zr alloys with high (3.3-3.6 wt%) lithium content, resulting a density reduction 12-14% and ultimate tensile stress ranging from 540 to 596 MPa. The corrosion resistance is also better (Fig.28) /37, 45/.

The high temperature alloys form these third group. These alloys contain transition metals at a high level (e.g. Al-Cu-Mn, Al-Fe-Mn, Al-Fe-Ce, Al-Fe-V-Si). The intermetallic compounds of these transition metals are stable even at higher temperatures and they hinder any grain boundary sliding, which [illegible]. ALLIED-SIGNAL Inc.'s new type of Al-Fe-V-Si powders have excellent mechanical properties due to the existence of a stable intermetallic compound in high volume fraction and homogeneous distribution /45/. In the USA there are several companies having the capability of commercially [illegible] aluminium alloy particulates: ALLIED-SIGNAL Inc. built a [illegible] plant, of 750,000 lb/year /45/, the TRANSMET Corp. (Columbus, [illegible]) has several melting machines rated at 50 metric tons per year and [illegible] of 2,000 metric tons per year each /144/.

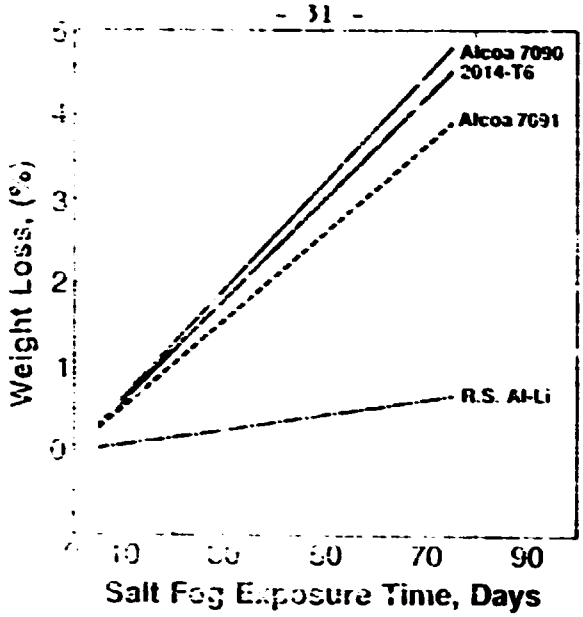

Fig.28. Salt spray corrosion rate of RS Al-Li alloy in comparison with conventional alloys /45/

Magnesium alloys. Nowadays the magnesium alloys are rarely used in the aerospace industry in spite of very low density (1.80-1.85 g/ml). Their poor mechanical properties and bad corrosion resistance have been improved by ALLIED-SIGNAL Inc. using a rapid solidification technology and new composition /45/. The RS magnesium alloy powders will probably find an increased application in automotive and aerospace industries /141/.

Titanium alloys. RS processing has been applied to both of conventional Ti-Al-V and novel alloys containing rare earth or metalloid intermetallic alloys /45/. There is a lot of results in improvement of high temperature mechanical properties but the application is still at the development stage. The problems are discussed by several authors /140, 141, 145/.

4.2.2 Tool and bearing materials. The tool steels contain a substantial amount of hard and brittle eutectic carbides which make their processing difficult. Since 1960 tool steels are produced by atomization and subsequent hot isostatic pressing in the USA, Sweden and Japan. The products have uniformly distributed fine carbide precipitates and small grain size. This microstructure results in more isotropic properties, improved thoughness and longer tool life. The commercialization is limited by their higher costs /62, 146/.

The [illegible] is also used to produce high performance materials [illegible] been mentioned in sec. 2.3.2. Ray reported /48-50/ on [illegible] chromium, tungsten alloys with low content of boron and carbon. By devitrification a very fine grained (about 0.2 μm) matrix has been [illegible] which was stabilized by boride and carbide precipitations about [illegible] μm size/. This alloys have high hot hardness and excellent

oxidation resistance at elevated temperatures up to 540 °C. In Table V. the high temperature hardness of microcrystalline and conventional tool steels is compared /147/.

Table V.

Hot Hardness Data After 30 Min. at Temperature

Alloy	Hot Hardness, HRC			
	Room Temperature	315°C	540°C	650°C
$Fe_{70}Cr_{18}Mo_2B_9Si_1$	44	43	43	42.5
AISI H21 steel (0.3C,0.4V,3.25Cr,9.5W, bal.Fe)	49.5	45	34.5	19
AISI H26 steel (0.55C,1.0V,4.0Cr,18W, bal.Fe)	46.5	42	32.5	20

Similar good results have been achieved by hot extrusion of ALLIED Corp.'s Devitrium 3065 and Devitrium 7025 type Ni-Mo-(Fe)-B alloys /148/.

4.2.3 Iron-based magnetic alloys. Although the amorphous soft magnetic alloys were in the spotlight of interest for many years, the RS processing is successfully applied both to conventional crystalline soft magnetic alloys (e.g. Fe-Si) and to the novel class of hard magnets (Fe-Nd-B), too /149/.

4.2.3.1 Soft magnetic alloys. Improvement of the traditional iron based soft magnetic materials (lower hysteresis loss, higher permeability and electrical resistivity) can be realized by increasing the content of non-magnetic components (Si or/and Al). Such materials produced by conventional technology, however, have very unconvenient mechanical properties: they are brittle, they can not be rolled or any machining can not be applied.

The technology of rapid quenching opens a new way for the development of soft magnetic materials. The improvement of the properties of the crystalline soft magnetic materials became possible immediately. This improvement is observable from two points of view an one hand the materials with traditional composition have better mechanical properties for machining and on the other hand, the magnetic and/or electrical properties of the alloys become better because this new techology makes it possible to increase the concentration of alloying elements.

Three alloy systems will be considered in more details Fe-Al, Fe-Si and Fe-Al-Si.

Fe-Al alloys. The magnetic properties of rapidly quenched materials may be improved significantly in some cases by heat treatment. Such a case is demonstrated in Fig.29 after Takanashi et al. /150/. In this figure hysteresis loops of a 15.4 w% Al content (a) and a 12.7 w% Al content (b) Fe-Al alloys are seen. The curves were measured in as-quenched state of the

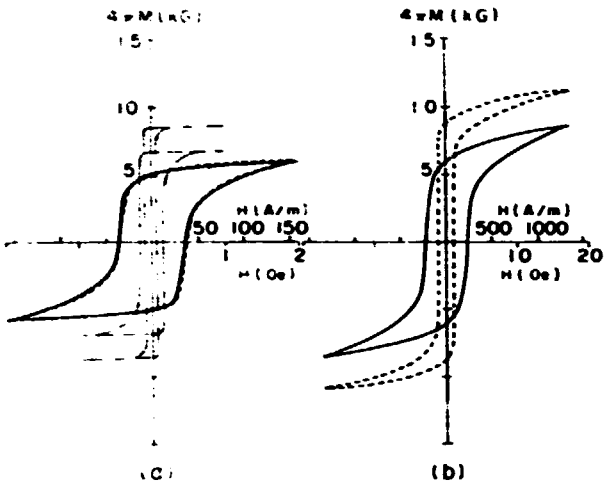

Fig.29.

d-c hysteresis loops for rapidly quenched (a) 15.4% Al-Fe alloy and the alloy in the Sendust region, and (b) 12.7% Al-Fe alloy. /150/

As-prepared (——) and after 800°C 1h annealing (- - -) for Fe-Al alloys.

As-prepared (——) and after 900°C 1h annealing (- - -) for Sendust.

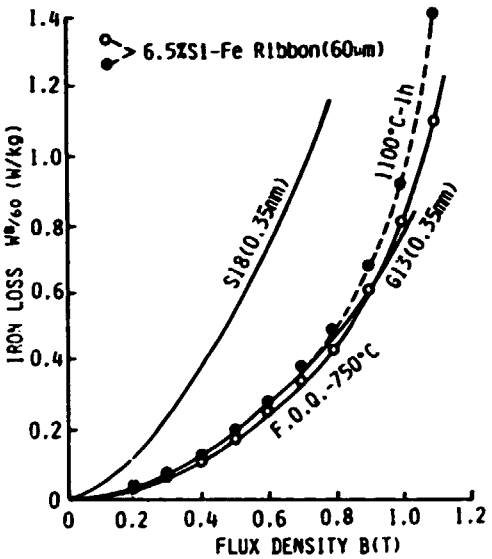

Fig.30. Iron loss per kg measured at 60 Hz as a function of the maximum flux density for various Si-Fe specimens after Narita /151/

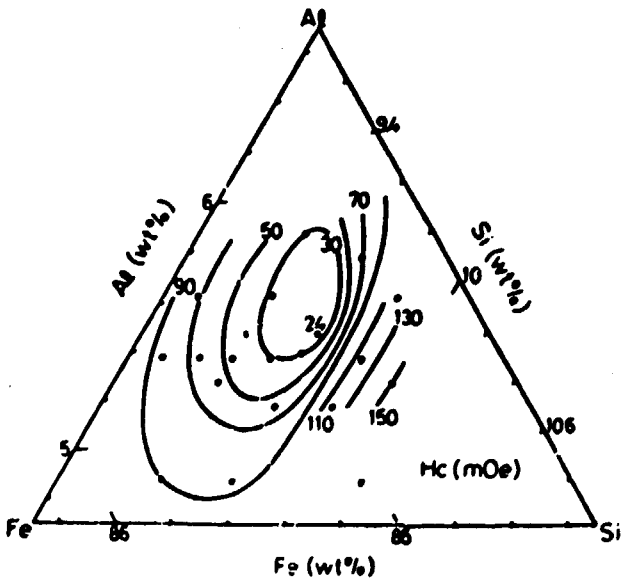

Fig.31. Concentration dependence of the coercive force H_c of Sendust ribbons in the cryst. state annealed at 835°C for 30 minutes in vacuum after Tsuya /152/

samples and after annealing at 800 ^{o}C for 1 hour. It is clearly seen that while in the case of (a.) practically there in no change, in the case of (b.) the heat treatment makes the magnetic properties better (coercive force decreases, remanence i.e. squareness increases). The Fe-Al alloys with 10-18 w% Al in rapidly quenched ribbon form have very good mechanical properties. 20-30 μm thick and 1.5 mm wide ribbons can be wounded around a rod with 1 mm diameter and they can be bent by 180^{o} /150/.

Fe-Si system. According to Narita /1 it is established that rapidly quenched Fe-Si alloys with about 6-7 w% Si have very good magnetic and mechanical properties. The thickness of the ribbons can be easily changed from 20 μm to 150 μm. In the as-quenched state they can be rolled and the majority of them can be bent by 180^{o}. With heat treatment at 1000-1100 ^{o}C for 1 hour an extremly soft material could be produced so that every ribbon could be bent by 180^{o}. The magnetic properties of rapidly quenched Fe-Si ribbons are also very good. A ribbon of 6.6 % Si content has a coercive force of 60 mOe after a heat treatment at 1180 ^{o}C for 1 hour. A sample with 80 mOe coercive force has 0.25 W/kg loss, which is less than the best quality commercially available textured 3 % Si-Fe sheet.

In Fig.30. we present, after Narita /151/, the losses of various Fe-Si materials in function of the flux density. Besides the results measured on a non-textured Fe-Si sheet, noted by (S18), and the textured sheet noted by (C13), the losses measured on ribbons produced by rapid quenching technology are shown. One of the ribbons was annealed at 1100 ^{o}C for 1 hour and then furnace cooled, the third one (F.O.Q) was heat treated at 750 ^{o}C and quenched into oil. It can be seen that the sample noted by (F.O.Q) has the lowest loss.

Fe-Al-Si system. Rapidly quenched materials in this ternary system exhibit similar properties as the binary systems mentioned before. After Tsuya /152/ in Fig.31. the coercive force of Fe-Al-Si alloys measured after annealing at 835 ^{o}C for 30 seconds is shown as a function of the concentration of the three components. The level line indicating the lowest coercive force corresponds to 30 mOe. The rapidly quenched Sendust ($Fe_{84.9}Si_{9.62}Al_{5.48}$) ribbon is ductile. It can be wound up around a rod 15 mm in diameter /152/.

Sendust alloys have found practical use in magnetic heads /153/ and other devices.

4.2 3.2 hard magnetic alloys. In the development of hard magnetic materials a sudden change was brought in by the application of rare earth transition metal alloys. This type of magnets has two peculiarities, one is that they are generally produced by powder metallurgy, the other is that initially high cobalt content materials were used (e.g. Co_5Sm). This increases the price of raw materials substantially.

In the last few years, however, in the course of application of rapid quenching technology a new type of hard magnetic materials was disovered (see

e.g. Croat et al. /46/) which resulted in the development of Fe-Nd-B hard magnetic materials. These magnets are produced both by melt spinning and traditional powder metallurgy /154/.

Besides their relatively low cost their advantage is the extreme high stored magnetic energy density $(BH)_{max}$. For commercially available magnets of this type, e.g. Neumax 35, produced by SUMITOMO SPECIAL MATERIALS Co. Ltd./Japan has $(BH)_{max}$=279 kJ/m^3. According to Wecker and Schultz /155/ rapidly quenched Nd-Fe-B magnets produced at optimal quenching parameters can reach a coercive force as large as 24 kOe, and a small amount of cobalt addition gives a further improvment of the coercivity /Fig.32/.

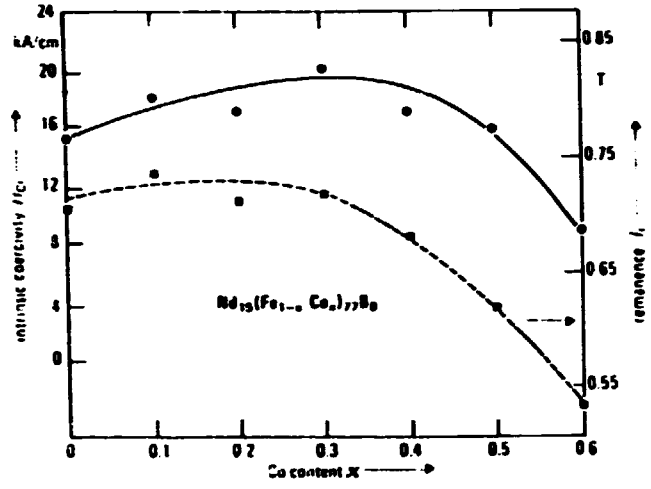

Fig.32. Coercivity H_{cI} and remanence J_r of optimally quenched ribbons vs Co content x /155/

During the last years the grinding into a powder of the melt-spun Nd-Fe-B ribbons became a prominent process with consecutive pressing of this powder in a bulk form using some fixative. This method has a great advantage because during pressing a magnetic field can be applied and in this way so higher quality anisotropic magnets can be produced. DELCO REMY, a Div. of GENERAL MOTORS is manufacturing Fe-Nd-B permanent magnets under the tradename MAGNEQUENCH® /47/.

4.2.4 Others. Rapid solidification processes have been applied in many other cases including nickel-based superalloys /156/, stainless steels /157/, copper based alloys /158/, etc. The majority of them did not reached the stage of manufacturing till now.

5 CONCLUSIONS

The development of the rapid solidification opened new possibilities for both of research and manufacturing.

The study of rapid solidification phenomena contributed to the understanding of the formation of solids under circumstances very far from the equilibrium. It became feasible to prepare novel types of microstructures (glassy or microcrystalline) and alloys having unusual compositions and properties.

The commercialization of the rapidly solidified alloys has been started. The excellent soft magnetic properties of metallic glasses are exploited in several devices as it was mentioned earlier (e.g. magnetic heads, shields, inductive components, ribbons for anti-thief systems, sensors). The use of flexible brazing and soldering foils is disseminated, too. Among the microcrystalline alloys the RS light metal alloys have found a practical use as structural materials in aerospace industry.

In spite of these results for the market penetration a relatively long time was needed. The commercialization of a new material is a complex process where not only the technical characteristics of the materials but other factors also have to be taken into account. These factors include the need for new manufacturing and design methods, the improvement of competitive materials, as well as economical considerations.

In the present applications the high-priced, high performance materials are in the focus e.g. the high strength light metal alloys for aerospace industry. This application is a rather limited field regarding e.g. the aluminium industry as a whole. Similar statement can be made related to high cobalt content amorphous soft magnets, too.

In 1987 Gilman estimated the annual production of rapidly solidified alloys to be about 10^5-10^6 kg per year /12/. It is really a very small part of the capacity of the metallurgical industry. But it is an eseential quantity if we take into account that the first ductile ferrous glasses were invented about 15 years ago. And it is an important point, that in many cases any improvement of the properties is not more possible by the traditional way.

The rapid solidification processes made possible the manufacturing of products with small cross sections, in this sense they meet the trend of development in modern metallurgy.

REFERENCES

/1/ M.C. Flemmings, Solidification Processing, McGraw Hill, New York, 1974

/2/ W. Klement, R.H. Willens, P. Duwez, Nature /London/ 187, /1960/ 869

/3/ H. Jones, Rapid Solidification of Metals and Alloys, The Institute of Metallurgists, London, 1982

/4/ R.E. Maringer, Mater. Sci. Engr. 98, /1988/ 13

/5/ R. Pond, Jr., R. Maddin, Trans. Met. Soc. AIME 245, /1969/ 2475

/6/ H.H. Liebermann, C.D. Graham, Jr., IEEE Trans. Magn. MAG-12, /1976/ 921

/7/ S. Kavesh, in: Metallic Glasses, ASM Metals Park, Ohio, USA, 1978, p. 36

/8/ H.H. Liebermann, J. Appl. Phys. 50, /1979/ 6773

/9/ H.H. Liebermann, R.L. Bye, Jr. in: Rapidly Solidified Crystalline Alloys, eds. S.K. Das, B.H. Kear, C.M. Adam, TMS, Warrendale, USA, 1985, p. 61

/10/ T.R. Anthony, H.E. Cline, ibid. 50, /1979/ 245

/11/ M.C. Narasimhan, US Patent 4,142,571 /1979/

/12/ J.J. Gilman, Phil. Trans. Royal Soc. London A 322, /1987/ 425

/13/ H.F. Hilzinger, K. Krueger, S. Hock, US Patent 4,386,648 /1983/

/14/ H. Fiedler, H. Mühlbach, G. Stephani, J. Mater. Sci. 19, /1984/ 3229

/15/ I. Nagy, C. Hargitai, Cs. Kopasz, Key Engineering Materials 13-15, /1987/ 857

/16/ A. Lovas, E. Kisdi-Koszó, L. Potocky, L. Novák, J. Mater. Sci. 22, /1987/ 1535

/17/ F. Vogt, G. Frommeyer, J.E. Wittig, H. Sassik, Mater. Sci. Engr. 98, /1988/ 295

/18/ W.J. Boettinger, ibid. 98, /1988/ 123

/19/ M.J. Tenwick, H.A. Davies, in: Rapidly Quenched Metals, eds. S. Steeb, H. Warlimont, North-Holland, Amsterdam, 1985, p. 67

/20/ F. Vogt, G. Frommeyer, ibid. p. 63

/21/ L. Granásy, Gy. Mészáros, ibid. p. 75

/22/ G. Stephani, H. Mühlbach, H. Fiedler, G. Richter, Mater. Sci. Engr. 98, /1988/ 29

/23/ J.C. Hubert, F. Mollard, B. Lux, Z. f. Metallkde 64, /1973/ 835

/24/ I. Gazsi, Y. Sahai, L.E. Hackman, in: Titanium Rapid Solidification Technology, eds. F.H. Froes, D. Eylon, TMS, Warrendale, USA, 1986, p. 69

/25/ [illegible] Kojiko, M. Yukumoto, S. Miyake, M. Ozawa, T. Kan, Mater. Sci. Engr. 98, /1988/ 25

/26/ [illegible] Kawakawa, Trans. Iron Steel Inst. Japan 26, /1986/ 3

/27/ [illegible] Mrowec, M. Jurisch, V.V. Maslov, W. Neumann, V.K. Nosenko, R. [illegible], G. Richter, ibid. 98, /1988/ 75

/28/ [illegible] Pimpaikar, R.S. Carbonara, J.J. Rayment, J.L. Mccall, A.H. Clauer, Am. Met. 19, p. 95

29. T. Masumoto, Int. J. Rapid Solidification 1, /1984-85/ 219

30. A. Inoue, T. Masumoto, I. Ogasawara, M. Hagiwara, in: Magnetic Properties of Amorphous Metals, eds. A. Hernando et al.,/Proc. Workshop, Sotalmádena, Spain, 1987/, North-Holland, Amsterdam, 1987, p. 117

31. M. Hagiwara, A. Inoue, T. Masumoto, Metall. Trans. 13A, /1982/ 373

32. A. Inoue, H. Tomioka, N. Yano, T. Masumoto, as Ref. 19., p. 1783

33. [illegible] L. Arnberg, N. Bäckstrom, S. Savage: Mater. Sci. Engr. 98, 1988 21

34. G. Naour, H.Bode, Wire Industry /March 1980/ p. 186

35. [illegible] Hawley, J. Metals 33, /Jan. 1981/ 13

36. N. [illegible] Grant: ibid. 35, /Jan. 1983/ 20

37. [illegible] Das, L.A. Davies: Mater. Sci. Engr. 98, /1988/ 1

38. J.E. Flinn: Rapid Solidification Technology for Reduced Consumption of Strategic Materials, Noyes Publications, Park Ridge, USA, 1985

39. H. Ravbould, C.F. Cline, as Ref. 9. p. 111

40. S. Hawley, K.B. Doherty, as Ref. 9. p. 77

41. [illegible] L. Arnberg, N. Bäckstrom, H. Klang, S. Savage, Mater. Sci. Engr. 98, 1988/ 43

42. [illegible] Laverania, N.J. Grant, ibid. 98, /1988/ 381

43. S. [illegible] Raman, A.N. Patel, R.S. Carbonara, Metal Powder Report 39, /1984/ 76

44. R.S. Carbonara, D.L. Erich, ibid. 42, /1987/ 53

45. Rapidly Solidified Alloys for High Performance Structural Applications, data sheets. ALLIED-SIGNAL Inc., Morristown, USA, 1987

46. [illegible] Croat, J.F. Herbst, R.W. Lee, F.E. Pinkerton, J. Appl. Phys. 55, 1984, 2078

47. MAGNEQUENCH^{R}, "rare earth" magnets, data sheets, DELCO REMY, Division of GENERAL MOTORS, Anderson, USA, 1987

48. R. Ray, Mater. Sci. Engr. 52, /1982/ 85

49. R. Ray, Engineers' Digest 43, /Aug. 1982/ 18

50. MARKOMET^{R}, new nickel base alloys made via rapid solidification, MARKO MATERIALS Inc., Billerica, USA, 1982

51. [illegible] W.M. Gibbon, R.S. Hollingshead, Mater. Sci. Engr. 98, /1988/ 41

52. [illegible] Kawamura, M. Takagi, M. Akai, T. Imura, ibid. 98, /1988/ 449

53. [illegible] Dunlop, L. Arnberg, ibid. 98, /1988/ 437

54. [illegible] R. Ray, P.J. Clemm, ibid. 98, /1988/ 395

55. [illegible] ibid 98, /1988/ 461

56. [illegible] Kawamura, M. Arakai, T. Kuroyama T. Imura, ibid. 98, 1988 457

57. [illegible] Mortlock, J. f. Werkstoffechn. 14, /1983/ 221

58. [illegible] Cobb, J. Sparagen, Mater. Sci. Engr. 98, /1988/ 325

59 [illegible] Nordin, H.W. Bergmann, in: Rapidly Solidified Metastable Materials eds. B.H. Kear, B.C. Giessen, North-Holland, New York, [illegible] p. 45

60 [illegible] Haseltine, R.W.K. Honeycombe, ibid. p. 65

61 [illegible] Tiemann, Mater. Sci. Engr. 69, /1985/ 95

62/ H. Jones, J. Mater. Sci. 19, /1984/ 1043

63/ F. Fouquet, E. Szmatula, Mater. Sci. Engr. 98, /1988/ 305

64/ J.C. Bittence, Materials Engr. 95, /1982/ 57

65/ M.R. Jackson, J.R. Rairden, J.S. Smith, R.W. Smith, J. Metals 33, /Nov. 1981/ 23

66 D. Turnbull, Contemp. Phys. 10, /1969/ 479

67 J.D. Fowlkes, J. Appl. Phys. 21, /1950/ 24

68 H.S. Chen, Rep. Prog. Phys. 43, /1980/ 375

69 P.H. Gaskell, J. Non-Cryst. Solids 32 /1979/ 207

70 G.S. Cargill, M.H. Cohen, Phys. Rev. B21, /1980/ 4113

71 F.E. Luborsky, in: amorphous Metallic Alloys, ed. F. Luborsky, Butterworths, London, 1983, p. 377

72 D. Turnbull, B.G. Bagley, in: Treatise on Solid State Chemistry, vol.5, ed. N.B. Hannay, Plenum Press, New York, 1975, p. 513

73 H.A. Davies as Ref. 71, p. 8

74 H.A. Davies, in: Rapidly Quenched Metals III., ed. B. Cantor, The Metals Society, London, 1978, vol.1, p. 1

75/ M.G. Scott, as Ref. 71, p. 144

76/ I.W. Donald, H.A. Davies, Phil. Mag. A42, /1980/ 277

77/ M. Naka, et. al., in: Rapidly Quenched Metals II., eds. N.J. Grant, B.C. Giessen, MIT Press, Cambridge, USA, 1976, vol.1, p. 273

78 P. Wang, Bull. Alloy Phase Diagrams 2, /1981/ 269

79 M.R.J. Gibbs, J.E. Evetts, I.A. Leake, J. Mater. Sci. 18, /1983/ 2

80/ R.C. O'Handley, as Ref. 71, p. 257

81 R. Hasegawa, R.C. O'Handley, J. Appl. Phys. 50, /1979/ 1551

82/ R.C. O'Handley, J. Appl. Phys. 62, /1987/ R15

83/ H. Kimura, T. Masumoto as Ref. 71, p. 187

84/ K. Hashimoto, as Ref. 19, p. 1449

85/ C. Yoon, D.L. Cocke, J. Non-Cryst. Sol. 79, /1986/ 217

86/ D.L. Cocke, J. Metals 38, /Febr. 1986/ 70

87/ D. Raskin, C.H. Smith, as Ref. 71, p. 381

88 J.J. Gilman, in: Frontiers in Materials Science, M.A. Meyers O.T. Inal, eds. Elsevier, Amsterdam, 1985 p. 175

89 [illegible] Flores, R. Carbonara, J. Metals 40, /Febr. 1988/ 20

90 [illegible], I. Kisdi-Koszó, A. Lovas, Report KFKI-1987-54/E pp.1-23, to be published in Physica Scripta /1988/

91 [illegible] Lachowicz, in: Amorphous Metals, eds., H. Matyja, P.G. Zielinski [illegible] World Scientific Publ. Co., Singapore, 1985 (Proc. Summer School, [illegible] Poland, 1985) p. 313

92 [illegible] Hilzinger, IEEE Trans. Magn. MAG-21, /1985/ 2020

95 [illegible] Ramanan, C.H. Smith, G.E. Fish, Key Engineering Materials [illegible] 1987 849

96 [illegible] Rosenfeld, in: Rapidly Solidified Materials, eds. P.W. Lee, R.J. Carbonara, ASM, Metals Park, USA, 1985 (Proc. Intl. Conf., San [illegible] USA, 1985) p. 427

97 H.F. Belder, ibid. p. 379

98 [illegible] Luborsky in: Glass-Current Issues, Martinus Nijhoff, BV, Dordrecht, Netherlands, 1985 (Proc. NATO Advanced Study Institute Conf.) p. 159

97 C.H. Smith, IEEE Trans. Magn. MAG-18, /1987/ 1376

98 G.E. Fish, C.H. Smith in: Soft and Hard Magnetic Materials with Applications, Choice Book Mfg. Co. Mars, USA, 1986, Paper 8617-002 pp. 1-20 (Proc. ASM Conf., Lake Buena Vista, USA, 1986/

99 METGLAS® Electromagnetic Alloys, technical bulletin, ALLIED Corp. METGLAS PRODUCTS, Parsippany, USA

100 N. Alexandrov, R. Schulz, R. Roberge, IEEE Trans. on Power Delivery PWRD-2, /1987/ 827

101 R. Schulz, N. Chretien, N. Alexandrov, J. Aubin, R. Roberge, Mater. Sci. Engr. 99, /1988/ 19

102 T. Kusnnick, D.L. Sawhney, R.E. Hathaway, US Patent 4,529,458 /1985/

103 D.M. Natnasingh, H.H. Liebermann, IEEE Trans. on Power Delivery PWRD-2, 1987 843

104 D.W. Whitley, ibid. PWRD-2, /1987/ 827

105 [illegible] Hatley, [illegible]A. Lowdermilk, A.C. Lee, J. Magn. Magn. Mater. 54-57, [illegible] 1616

106 METGLAS® products for Pulse Power, technical bulletin, ALLIED Corp., METGLAS PRODUCTS, Parsippany, USA

107 Zhang Luo, Liu Guang-Di, Song-Yao as Ref.19, vol.II. p. 1679

108 R. Boll, H.R. Hilzinger, Elektronik /Oct. 1987/ p. 99

109 G. Gratzer, J. Magn. Magn. Mater. 9, /1978/ 91

110 HITACHI Amorphous Alloys "ACO" and "ACO-S", Wound Cores for Control Reactor, Hitachi Metals Reports, No.E221 pp.1-7, HITACHI AMETALS, Ltd., Tokyo, Japan

111 Amorphous Metals - Toroidal strip cores of VITROVAC® 6025 and 6030, technical bulletin No.VC 004, VACUUMSCHMELZE GmbH, Hanau, FRG

112 G.E. Fish, J. Physique 46, /1985/ C6-207

113 Y. Mazino, as Ref.19, vol.II. p. 1699

114 [illegible] Rotter, Funkschau 57, /1985/ 42

115 [illegible] de Wit, [illegible] Jager, Philips Techn. Rev. 44, /1988/ 101

116 [illegible] Magnetic Head, data sheet, MATSUSHITA ELECTRIC, Carson, USA

117 [illegible] Beaumont, P. Boll, J. Magn. Magn. Mater. 26, /1982/ 97

118 [illegible], Elektronik 31, /1982/ 43

119 [illegible] Hsiao, Wen-Hua How, Pei-Chih Yao, Shu-Fu Hsu, J. Appl. Phys. [illegible]

120 [illegible] IEEE Trans. Magn. Magn. MAG-20, /1984/ 942

121 [illegible], as Ref.19, vol.II. p. 1687

122 METGLAS® Flexible Brazing Foils, data sheets, ALLIED Corp. METGLAS PRODUCTS Partsippany, USA

123 [illegible] DeCristofaro C. Henschel, Welding Journal /July 1978/ p. 33

124 N. J. DeCristofaro, A. Datta, as Ref.19, vol.II. p. 1715

125 N.J. DeCristofaro, A. Datta, as Ref.9, p. 263

126 [illegible] Ackermann, P. Fournier, in: Proc. 4th International Conf. on Rapidly Quenched Metals, eds. T. Masumoto, K. Suzuki, The Japan Inst. Metals, Sendai, 1981, p. 1407

127 P. Nagyari, Concrete with glass metal reinforment, Proc. 13th Congress of International Assoc. for Bridge and Structural Engr., Helsinki, Finland, June 1988, p. 21

128 K. Asami, A. Kawashima, K. Hasimoto, Mater. Sci. Engr. 99, /1988/ 475

129 M.C. Flemings, Y. Shionara, Trans. Iron Steel Inst. Japan 26, /1986/ 6

130 H.W. Bergmann, H.U. Firtsch as Ref. 59, p. 3

131 M. Cohen, B.H. Kear, R. Mehrabian, in: Rapid Solidification Processing: Principles and Technologies, II, eds. R. Mehrabian, B.H. Kear, M. Cohen, Claitor's Publ. Div., Baton Rouge, USA, 1980, p. 1

132 Undercooled Alloy Phases, eds. E.W. Collings, C.C. Koch, TMS, Warrendale, USA, 1986

133 W.J. Boettinger, J. H. Perepezko, as Ref.9, p. 21

134 M.J. Aziz, J. Appl. Phys. 53, /1982/

135 H. Jones, Mater. Sci. Engr. 65, /1984/ 145

136 C.J. Baker, W.J. Cahn, Acta Metall. 17, /1969/ 575

137 H.W. Gilmer, Mater. Sci. Engr. 65, /1984/ p. 15-25

138 V.I. Borisov, Soviet Phys. Dokl. 7, /1962/ 50

139 I.W. Boettinger, R.S. Coriell, F.R. Sekerka, Mater. Sci. Engr. 65, /1984/ 27

140 E. Lavernia, B. Poggiali, I. Servi, J. Clark, F. Katrak, N. Grant, J. Metals /Nov. 1985/ 35

141 F.H. Froes, Y.-W. Kim, F. Hehmann, ibid. /Aug. 1987/ 14

142 P.R. Pickens, J.S. Ahearn, R.O. England, D.C. Cooke, in: High Strength Powder Metallurgy Aluminium Alloys II., eds. G.J. Hildeman, M.J. Koczak, TMS, Warrendale, USA, 1986, p. 105

143 R.E. Lewis, E.A. Starke, Jr., in: Mechanical Behaviour of Rapidly Solidified Materials, eds. S.M.L. Sastry, B.A. MacDonald, TMS, Warrendale, USA, 1985, p. 151

144 TRANSMET Facilities and Capabilities, technical information no. TM-70., TRANSMET Corp., Columbus, USA, 1986

145 F.H. Froes, R.G. Rowe, as Ref. 24 p. 1

146 [illegible] P.G. Bourdeau, as Ref. 9, p. 185

147 [illegible] J. Metals 34, /June 1982/ p. 1

148 [illegible] Whitmer, T.P. Whelan, G.I. Stapleton as Ref. 9, p. 541

149 [illegible] K. Hasegawa, as Ref. 9, p. 245

150 M. [illegible], T. Miyazaki, T. Watanabe, S. Ishio, Jpn. J. Appl. Phys. [illegible]

[illegible] N. Ieshima, Y. Yamashiro, Y.J. Shin, Y. Yoshida, J. Magn. Mag. Mater. 54 1984. 86

152 [illegible] Arai, J. Appl. Phys. 50,/1979/ 1658

153 M. Tsuya, et al. IEEE Trans. Magn. MAG-17, /1981/ 3111

154 E.A. Nitscheil, ed., Nd-Fe Permanent Magnets: Their Present and Future Applications, Elsevier Applied, Science Publishers, London, 1985

155 J. Wecker, L. Schultz, Appl. Phys. Lett. 51, /1987/ 697

156/ A.E. Laub, M.R. Jackson, S.C. Huang, E.L. Hall, as Ref. 59 p. 389

157/ G.F. North, F.E. Flinn, as Ref. 143, p. 85

158 I.E. Anderson, B.B. Rath, as Ref. 9, p. 219

Appendix I.

SOURCES OF INFORMATION ON RAPID SOLIDIFICATION

1. International journals

International Journal of Rapid Solidification
Materials Science and Engineering
Journal of Non-Crystalline Solids
Journal of Magnetism and Magnetic Materials
Journal of Materials Science
Journal of Metals
Materials Science Letters
Metal Powder Report etc.

2. Bibliographies

Rapidly Quenched Metals: A Bibliography 1973-1979, C. Suryanarayana, IFI/Plenum Press, New York, 1980

Amorphous Magnetism and Metallic Magnetic Materials-Digest. Survey of the Literature with a Complete Bibliography, A.R. Ferchmin, S. Kobe, eds., North-Holland, Amsterdam, 1983

3. Monographs

Metallic Glasses, American Soc. for Metals, Metals Park, Ohio, USA, 1979

Glassy Metals vol.I., H.J. Güntherodt, H. Beck, eds., Springer Verlag, Berlin 1981

Glassy Metals vol.II., H. Beck, H.J. Güntherodt, eds Springer Verlag, Berlin, 1983

Metallic Glasses: Magnetic, Chemical and Structural Properties, R. Hasegawa, ed., CRC, Boca Raton, 1983

Amorphous Metallic Alloys, F.E. Luborsky, ed., Butterworths, London, 1983

Metallic Glasses: Production, Properties and Applications, T.R. Anantharaman, ed., Trans. Tech. Publ., 1984

4. Conferences and symposia proceedings

International Conferences on Rapidly Quenched Metals (RQ)

RQ-1: Proc. of the International Conference on Metastable Metallic Alloys, Brela, Yugoslavia, 1970, FIZIKA, vol.2. Suppl.2. /1970/

RQ-2: Proc. of the 2nd International Conference on Rapidly Quenched Metals, Boston, USA, 1975, N.J. Grant, B.C. Giessen, eds., MIT Press, Cambridge, Mass. 1977 (Section I.), Section II.: Mater. Sci. Engr. 23 /1976/

RQ-3: Rapidly Quenched Metals III. eds., B. Cantor, Metals Society, London, 1978

RQ-4: Proc. 4th Int. Conf. on Rapidly Quenched Metals (Sendai, Japan, 1981) vol. 1-2, T. Masumoto, K. Suzuki, eds., the Japan Inst. Metals, Sendai, 1981

RQ-5: Rapidly Quenched Metals, Würzburg, FRG, 1984, vol. I.-II., S. Steeb, H. Warlimont, eds., North-Holland, Amsterdam, 1985

RQ-6: Rapidly Quenched Metals, Montréal, Canada, 1987, vol. I.-III., H. Cochrane, J. Strom-Olsen, eds., Mater. Sci. Engr. 98-100, /1988/

Rapid Solidification Processing: Principles and Technologies, R. Mehrabian et al. eds., Claitor's Publ. Div., Baton Rouge, USA, 1978 (Proc. First. Int. Conf., Reston, USA, 1977)

Rapid Solidification Processing: Principles and Technologies II., R. Mehrabian, B.H. Kear, M. Cohen, eds., Claitor's Publ. Div., Baton Rouge, USA, 1980 (Proc. Second Int. Conf., Reston, USA, 1980)

Rapid Solidification Processing: Principles and Technologies III., R. Mehrabian, ed., NBS, USA, 1983 (Proc. Third Int. Conf., Gaithersburg, USA, 1982)

F.S. Machlin, T.J. Rowland, eds., Synthesis and Properties of Metastable Phases, TMS-AIME, Warrendale, USA, 1980 (Proc. Symp. Pittsburgh, USA, 1980)

Continuous Casting of Small Cross Sections, Y.V. Murty, F.R. Mollard, eds. The Metallurgical Soc. of AIME, Warrendale, USA, 1981 (Proc. Symp. Pittsburgh, USA, 1980)

Rapidly Solidified Amorphous and Crystalline Alloys, B.H. Kear, B.C. Giessen, M. Cohen, eds., North-Holland, New York, 1982 (Proc. Symp., Boston, USA, 1981)

Chemistry and Physics of Rapidly Solidified Materials, B. Bendow, R.O. Scattergood, eds., TMS-AIME, Warrendale, USA, 1983 (Proc. Symp. St. Louis, USA, 1983)

Rapidly Solidified Metastable Materials, B.H. Kear, B.C. Giessen, eds., North-Holland, New York, 1984 (Proc. Symp. Boston, USA, 1983)

Rapidly Solidified Alloys and Their Mechanical and Magnetic Properties,
B.C. Giessen, D.E. Polk, A.I. Taub, eds., MRS, Pittsburgh, USA, 1986 (Proc. Conf., Boston, USA, 1985)

Rapidly Solidified Materials, P.W. Lee, R.S. Carbonara, eds., ASM, Metals Park, Ohio USA, 1985 (Proc. Int. Conf., San Diego, USA, 1985)

Titanium: Rapid Solidification Technology, F.H. Froes, D. Eylon, eds., TMS-AIME, Warrendale, USA, 1986 (Proc. Symp., New Orleans, USA, 1986)

Mechanical Behavior of Rapidly Solidified Materials, S.M.L. Sastry, P.A. MacDonald, eds., TMS-AIME, Warrendale, USA, 1986 (Proc. Conf., New York, USA, 1985)

Magnetic Properties of Amorphous Metals, A. Hernando et al., eds. North-Holland, Amsterdam, 1987 (Proc. Symposium, Benalmádena, Spain, 1987)

Appendix II.

List of RS PRODUCTS and MANUFACTURERS

Manufacturer	Product
1. ALLIED Corp. (formerly ALLIED CHEMICAL CORP.) METGLAS PRODUCTS, Parsippany, NJ, USA	METGLAS^{R} amorphous alloys a.) soft magnetic ribbons b.) ductile brazing foils METSHIELD^{R} flexible magnetic shields
ALLIED-SIGNAL Inc., Morristown, NJ, USA	RS aluminium- and magnesium based alloys for structural application
2. DELCO REMY, Div. of GENERAL MOTORS, Anderson, IN, USA	MAGNEQUENCH^{R} "rare earth" hard magnets
3. FIBRE TECHNOLOGY Ltd., Somercotes, UK	RS alloys in form of wires, sheets, fine particulate
4. HITACHI METALS Ltd., Tokyo, Japan	soft magnetic amorphous ribbons typ. ACO and ACO-S, wound cores for control reactor
5. MARKO MATERIALS Inc., Billerica, MA, USA	MARKOMET^{R} alloys: RS powders for plasma spraying and compaction
6. MATSUSHITA ELECTRIC Corp. of AMERICA, Secaucus, NJ, USA	amorphous magnetic heads
7. RIBTEC RIBBON TECHNOLOGY Corp., Gahanna, OH, USA	RIBTEC MO typ. metal fibers and wire for reinforcing composites
8. TRANSMET Corp., Columbus, OH, USA	RS aluminium alloy particulates
9. UNITIKA Ltd., Osaka, Japan	amorphous and microcrystalline wires
10. VACUUMSCHMELZE GmbH, Hanau, FRG	VITROVAC^{R} soft magnetic amorphous